ACOUSTICAL RADIATION FROM PERIODICALLY STIFFENED MEMBRANE EXCITED BY TURBULENT BOUNDARY LAYER

Yi Mason Chang

Massachusetts Institute of Technology

Prepared for:

David W. Taylor Naval Ship Research and Development Center

April 1975

ACOUSTICAL RADIATION FROM PERIODICALLY STIFFENED MEMBRANE EXCITED BY TURBULENT BOUNDARY LAYER

by

YI MASON CHANG

Report No. 70208-11

This research was carried out under the Naval Ship Systems Command General Hydromechanics Research Program Subproject SR 009 01 01, administered by the Naval Ship Research and Development Center Contract N00014-67-A-0204-0002

Approved for public release; distribution unlimited.

ACOUSTIC AND VIBRATION LABORATORY
Massachusetts Institute of Technology
Cambridge, Massachusetts 02139

Technical Report No. 70208-11

ACOUSTICAL RADIATION FROM PERIODICALLY STIFFENED MEMBRANE EXCITED BY TURBULENT BOUNDARY LAYER

by

Yi Mason Chang

This research was carried out under the Naval Ship Systems Command General Hydromechanics Research Program Subproject SR 009 01 01, administered by the Naval Ship Research and Development Center. Approved for public release; distribution unlimited.

April 1975

Acoustics and Vibration Laboratory
Massachusetts Institute of Technology
Cambridge, Massachusetts 02139

UNCLASSIFIED

SECURITY CLASSIFICATION OF THIS PAGE (When Data Entered)

REPORT DOCUMENTATION PAGE		READ INSTRUCTIONS BEFORE COMPLETING FORM
1. REPORT NUMBER 70208-11	2. GOVT ACCESSION NO.	3. RECIPIENT'S CATALOG NUMBER
4. TITLE (and Subtitle) Acoustical Radiation from Periodically Stiffened Membrane Excited by Turbulent Boundary Layer		5. TYPE OF REPORT & PERIOD COVERED Interim Report February 1973--August 1974 6. PERFORMING ORG. REPORT NUMBER
7. AUTHOR(s) Yi Mason Chang		8. CONTRACT OR GRANT NUMBER(s) N00014-67-A-0204-0002
9. PERFORMING ORGANIZATION NAME AND ADDRESS Massachusetts Institute of Technology Cambridge, Massachusetts 02139		10. PROGRAM ELEMENT, PROJECT, TASK AREA & WORK UNIT NUMBERS SR009 01 01
11. CONTROLLING OFFICE NAME AND ADDRESS Naval Ship Research and Development Center Bethesda, Maryland 20034		12. REPORT DATE April 1975 13. NUMBER OF PAGES 81
14. MONITORING AGENCY NAME & ADDRESS(if different from Controlling Office)		15. SECURITY CLASS. (of this report) Unclassified 15a. DECLASSIFICATION/DOWNGRADING SCHEDULE NA

16. DISTRIBUTION STATEMENT (of this Report)

This document has been approved for public release and sale, its distribution is unlimited.

17. DISTRIBUTION STATEMENT (of the abstract entered in Block 20, if different from Report)

18. SUPPLEMENTARY NOTES

19. KEY WORDS (Continue on reverse side if necessary and identify by block number)

Acoustic Radiation
Stiffened Membrane
Turbulent Boundary Layer
Wall Pressure Fluctuation

20. ABSTRACT (Continue on reverse side if necessary and identify by block number)

Characteristics of periodically stiffened membrane are studied by using a string model loaded with equally-spaced mass and rotary inertia. The acoustical radiation by periodically stiffened membrane excited by a turbulent boundary layer is estimated using a modal analysis on an individual bay of membrane between stiffeners.

Two theoretical predictions of radiated sound power are made using statistical energy methods. One is based upon measured wall pressure data,

DD FORM 1 JAN 73 1473 EDITION OF 1 NOV 65 IS OBSOLETE
S/N 0102-014-6601

UNCLASSIFIED

SECURITY CLASSIFICATION OF THIS PAGE (When Data Entered)

the other upon measured vibratory response of the membrane. Both agree well with direct measurements of radiated sound power.

ic

ACOUSTICAL RADIATION FROM PERIODICALLY STIFFENED MEMBRANE EXCITED BY TURBULENT BOUNDARY LAYER

by

Yi Mason Chang

ABSTRACT

Characteristics of periodically stiffened membrane are studied by using a string model loaded with equally-spaced mass and rotary inertia. The acoustical radiation by periodically stiffened membrane excited by a turbulent boundary layer is estimated using a modal analysis on an individual bay of membrane between stiffeners.

Two theoretical predictions of radiated sound power are made using statistical energy methods. One is based upon measured wall pressure data, the other upon measured vibratory response of the membrane. Both agree well with direct measurements of radiated sound power.

TABLE OF CONTENTS

NOMENCLATURE

b	Dimension of the cross section of stiffener
$C_{m,n}$	Membrane wave speed for (m,n) mode
C_o	Acoustic wave velocity
f	Frequency
k_1	Wave vector in ℓ_1-direction
k_3	Wave vector in ℓ_3-direction
ℓ_1	Spacing between stiffeners
ℓ_3	Transverse membrane dimension
m	Membrane area density
N	Number of stiffeners plus one (=10)
n_s	Frequency modal density
p	Wall pressure
P	Acoustic pressure radiated by membrane
T_m	Membrane tension
U_c	Convection velocity
U_∞	Free stream velocity
Z	Radiation impedance
$\phi(\omega)$	Wall pressure spectral density
η	Loss factor
ρ	Fluid (air) density
π	Spectral density of radiated acoustic power
σ	Membrane area density
ω	Angular frequency

I. INTRODUCTION

Much work has been done on the vibratory response of thin plates or membranes to a turbulent boundary layer pressure excitation and the subsequent radiation of sound by these plates or membranes. In the previous work, studies have included only the response of, or radiation from, simple structures. Actual structures may be a complex system of plates forming a skin over a rib-like structure of beams. In one limit, very rigid beams divide the skin into a number of adjacent bays: the response of such structures can be modeled by treating the response of each bay separately. Generally, however, the beams are not infinitely rigid, and we must consider the combined response of ribs and skins. To understand the response of such systems, in the present study we investigate the response and radiation of a periodically stiffened membrane.

The characteristics of the membrane and stiffeners system are studied by using a one-dimensional string model carrying equally-spaced blocks having mass as well as rotary inertia. The analysis used here is similar to that used by J. W. Miles.[1] The natural frequencies fall in periodically-spaced groups, the lower ends of which correspond, at high frequency, with the natural frequencies of each of the string segments between the blocks and with the blocks fixed as rigid supports.

The radiated acoustic power from the periodically stiffened membrane excited by turbulent boundary layer is

estimated using a modal analysis on an individual bay of membrane between stiffeners. The contributions of Lyon and Maidanik,[2] Leehey,[3] Davies,[4] and many others, have provided a broad fundamental theoretical basis upon which this part of the study develops. The analysis is based on an expansion of the transverse velocity field of the membrane bay in terms of orthogonal characteristic functions. It is assumed throughout the analysis that the response of the membrane at any frequency is determined by the response of those modes which are resonantly excited at, or near to, that frequency. This assumption is justified for the cases of turbulent boundary layer excited structures when the correlation lengths of the exciting field are small compared to the panel dimension. Then, expressions for the acoustic power radiated in narrow bands of frequencies can be obtained by summing over those modes that have resonant frequencies within the band by making use of the statistical energy analysis (SEA) assumption of equal energy among the modes.

Corcos's[5] model of the wall-pressure correlation function is used to obtain the modal wall-pressure spectral densities. Values of the modal radiation coefficients for plates have been calculated by Davies.[4] His results are applied here to the cases of membranes.

II. CHARACTERISTICS OF PERIODICALLY-STIFFENED MEMBRANE

The equation of motion for a membrane can be written in the form

$$\left(\frac{\partial^2}{\partial x^2} + \frac{\partial^2}{\partial z^2}\right) h = \frac{\sigma}{T_m} \frac{\partial^2 h}{\partial t^2}$$

where T_m is membrane tension, σ the area mass density of the membrane, $h(x,z,t)$ the normal displacement of the membrane, x-coordinate is in the longitudinal direction of membrane. z-coordinate is in the lateral direction of membrane, and is parallel with the axes of the stiffeners.

Note that, if we let h assume a form of $h=X(x)Z(z)e^{i\omega t}$ where X and Z are respectively functions of x and z only then we can easily decompose the equation of motion into two uncoupled one-dimensional equations:

$$\frac{\partial^2 X}{\partial x^2} + k_1^2 X = 0$$

$$\frac{\partial^2 Z}{\partial z^2} + k_3^2 Z = 0$$

where $k_1^2 + k_3^2 = k^2 = \omega^2/C_m^2$, $C_m = \sqrt{T_m/\sigma}$ being the membrane wave speed.

By tapering the ends of the stiffeners, and by knowing that the levels of vibrations and rotations of the membrane system are small, we can approximate the longitudinal characteristics of this system by that of a string, carrying equally-spaced blocks of mass and rotary inertia resting on elastic foundation. For simplicity, the elastic foundation is represented by two springs, each of stiffness S/2, for each block as shown in Figure 2.1. The equation of motion of the string is

$$\frac{\partial^2 y}{\partial x^2} + k_1^2 y = 0 \qquad (2.1)$$

where we use $y(x,t)$ as the displacement of the string.

In the formulation of the boundary value problem for this periodical structure, we also find it convenient to introduce

a dimensionless, local coordinate such that

$$y = \ell_1 y_n(\xi) \quad , \quad n = 1,2,\ldots,N \tag{2.2a}$$

$$\xi = \frac{x-dn}{\ell_1}, \quad d_n \leq X \leq d_n+\ell \quad \text{and} \quad d_n = (n-1)(\ell_1+b) \tag{2.2b}$$

where N is the number of string segments separated by stiffeners, i.e., the number of stiffeners plus one, ℓ_1 is the spacing between stiffeners. In addition, let

$$\lambda^2 = k_1^2 \ell_1^2 \tag{2.3}$$

Note the λ is also a dimensionless eigenvalue parameter. Now, Eq.(2.1) becomes

$$\frac{\partial^2 y_n}{\partial \xi^2} + \lambda^2 y_n = 0 \qquad n = 1,2,\ldots,N \tag{2.4}$$

Let us study the equilibrium conditions associated with block number (n-1). We assume that all angles are very small. Equilibrium of force in vertical direction is thus

$$\left(\frac{\partial y_n(0)}{\partial \xi} - \frac{\partial y_{n-1}(1)}{\partial \xi}\right) = \frac{\ell_1}{T} \frac{S-\omega^2 M}{2}\left\{y_{n-1}(1) + y_n(0)\right\} \tag{2.5a}$$

where M is the mass of one stiffener, $T = T_m \ell_3$, and

$$n = 2,3,\ldots,N.$$

Assuming θ_b very small, the equilibrium of momentum with respect to the center of the block can be written in the form

$$-T(b \sin \theta_b + b \cos \theta_b) + \left(\frac{S\ell_1}{2} y_{n-1}(1) + T \frac{\partial y_{n-1}(1)}{\partial \xi}\right)(b \cos \theta_b - b \sin \theta_b)$$

$$+T(-b \sin \theta_b + b \cos \theta_b) + \left(-\frac{S\ell_1}{2} y_n(0) + T\frac{\partial y_n(0)}{\partial \xi}\right)(b \cos \theta_b + b \sin \theta_b) = I\ddot{\theta}_b$$

or

$$\left(\frac{\partial y_{n-1}(1)}{\partial \xi} - \sin \theta_b\right) + \left(\frac{\partial y_n(0)}{\partial \xi} - \sin \theta_b\right) + \sin \theta_b \left(\frac{\partial y_n(0)}{\partial \xi} - \frac{\partial y_{n-1}(1)}{\partial \xi}\right)$$

$$- \frac{S\ell_1}{2T} \sin \theta_b \left(\frac{2b}{\ell_1} + y_{n-1}(1) + y_n(0)\right) = \frac{I\ddot{\theta}_b}{Tb}$$

where 2b is the dimension of the block. On the left-hand side of the above equation, the third term is much smaller in magnitude than the first two terms, and, hence, is negligible. Also, remember that Θ_b is very small Now, the equation goes over to

$$-2\Theta_b + \left(\frac{\partial y_{n-1}(1)}{\partial \xi} + \frac{\partial y_n(0)}{\partial \xi}\right) - \frac{Sb}{T}\Theta_b = \frac{I}{Tb}\ddot{\Theta}_b \qquad n = 2,3,\ldots,N$$

Since the forcing functions of the above differential equations, $\partial y_{n-1}(1)/\partial \xi$ and $\partial y_n(o)/\partial \xi$, have harmonic time dependence of ω, $\ddot{\Theta}_b$ can be replaced by $-\omega^2\Theta_b$. Also, note that $y_n(o) - y_{n-1}(1) = \frac{2b}{\ell_1}\Theta_b$; n = 2,3,...N. Thus, we have

$$-y_{n-1}(1) + y_n(0) = \frac{2b}{\left(2-\frac{I\omega^2}{Tb}+\frac{Sb}{T}\right)\ell_1}\left(\frac{\partial y_{n-1}(1)}{\partial \xi} + \frac{\partial y_n(0)}{\partial \xi}\right) ; \qquad n = 2,3,\ldots,N \qquad (2.5b)$$

On the ends of the string, we have

$$y_1(0) = 0 \qquad (2.5c)$$

$$y_N(1) = 0 \qquad (2.5d)$$

The most general solution to Eq.(2.4) is

$$y_n(\xi) = A_n \sin \lambda\xi + B_n \cos \lambda\xi \; ; \; n = 1,2,\ldots,l. \qquad (2.6)$$

Now, Eq.(2.5a) and Eq.(2.5b) give, respectively

$$\alpha[B_n + A_{n-1} \sin \lambda + B_{n-1} \cos \lambda] = A_n - A_{n-1} \cos \lambda + B_{n-1} \sin \lambda \qquad (2.7a)$$

$$\beta[B_n - A_{n-1} \sin \lambda - B_{n-1} \cos \lambda] = A_n + A_{n-1} \cos \lambda - B_{n-1} \sin \lambda \qquad (2.7b)$$

where

$$\alpha = \frac{(S-M\omega^2)\ell_1}{2T\lambda}$$

$$\beta = \frac{\left(1+\frac{sb}{2T} - \frac{I\omega^2}{2Tb}\right)\ell_1}{b\lambda}$$

$$n = 2,3,\ldots,N$$

Eq.(2.7a) subtracted from (2.7b) gives

$$A_{n-1} = \frac{-(\alpha-\beta)B_n+[-(\alpha+\beta)\cos\lambda+2\sin\lambda]B_{n-1}}{(\alpha+\beta)\sin\lambda+2\cos\lambda} \; ; \; n = 2,3,\ldots,N \tag{2.8a}$$

Eq.(2.7a) added to (2.7b) gives

$$A_n = \frac{(\alpha-\beta)B_{n-1}+[(\alpha+\beta)\cos\lambda+2\alpha\beta\sin\lambda]B_n}{(\alpha+\beta)\sin\lambda+2\cos\lambda} \; ; \; n = 2,3,\ldots,N \tag{2.8b}$$

Substitution of A_n and A_{n-1} in the form of Eq.(2.8a) back into Eq.(2.7a) gives

$$B_{n+1} - 2ZB_n + B_{n-1} = 0 \; ; \; n = 2,3,\ldots(N-1) \tag{2.9}$$

where

$$Z = \frac{(\alpha\beta-1)\sin\lambda+(\alpha+\beta)\cos\lambda}{\beta-\alpha} \tag{2.9a}$$

The most general solution to Eq.(2.9) is given by

$$B_n = A\sin(n\theta) + B\cos(n\theta) \tag{2.10}$$
$$Z = \cos\theta$$

where A and B are arbitrary constants. From Eqs.(2.5c), (2.6), and (2.10), we get

$$B_1 = A\sin\theta + B\cos\theta = 0 \tag{2.10a}$$

Similarly, from Eqs.(2.5d), (2.6), and (2.8b), we have

$$\frac{(\alpha-\beta)B_{N-1}+[(\alpha+\beta)\cos\lambda+2\alpha\beta\sin\lambda]B_N}{(\alpha+\beta)\sin\lambda+2\cos\lambda}\sin\lambda + B_N\cos\lambda = 0$$

or, after simplification,

$$(\alpha-\beta)B_{N-1}\sin\lambda + 2B_N(\cos\lambda+\alpha\sin\lambda)(\cos\lambda+\beta\sin\lambda) = 0$$

or,

$$A[(\alpha-\beta)\sin\lambda\sin(N-1)\theta+2\sin N\theta(\cos\lambda+\alpha\sin\lambda)(\cos\lambda+\beta\sin\lambda)]$$
$$+B[(\alpha-\beta)\sin\lambda\cos(N-1)\theta+2\cos N\theta(\cos\lambda+\alpha\sin\lambda)(\cos\lambda+\beta\sin\lambda)]$$
$$= 0 \tag{2.10b}$$

From Eqs.(2.10a) and (2.10b), we have

$$(\alpha-\beta)\sin\lambda\sin(N-2)\theta+2(\cos\lambda+\alpha\sin\lambda)(\cos\lambda+\beta\sin\lambda)\sin(N-1)\theta=0 \qquad (2.11)$$

From Eq.(2.10), we see $Z = \cos\theta$, where θ is real when $|Z|$ is equal or less than one, and θ is imaginary when $|Z|$ is greater than one. It is easy to see that when θ is real, we will be able to solve for eigenvalues from Eq.(2.11). If θ is imaginary, say, $\theta = iX$, with X real, Eq.(2.11) becomes

$$(\alpha-\beta)\sin\lambda\sinh(N-2)X+2(\cos\lambda+\alpha\sin\lambda)(\cos\lambda+\beta\sin\lambda)\sinh(N-1)X = 0 \qquad (2.11b)$$

A little calculation shows that, for large value of λ, $(\alpha-B)\sin\lambda$ is less than $2(\cos\lambda+\alpha\sin\lambda)(\cos\lambda+\beta\sin\lambda)$. Besides, we know $\sinh(N-1)X$ is larger than $\sinh(N-2)X$. Thus, it is impossible to find a solution of λ which makes $|Z|>1$ and, at the same time, satisfies Eq.(2.11b). So, we see the resonant frequencies are permitted only within bands where $|Z|\leq 1$ or θ is real, as shown in Figure (2.2). Note that at high frequency the asymptotic approximation of Z is $Z \sim C\lambda\sin\lambda$, where $C = IM/(M - I/b^2)\ 2\ell_1 b^2$. A computer analysis shows the resonant frequencies as listed in Table 2.1. Notice that in each frequency band there are ten resonant modes. We applied Lagrangian energy method to the system with a simplification that the strings are massless. We found two natural frequency bands comparable to the first two bands listed in Table 2.1, and that the first band involves mainly the heaving and the second the rotating of the blocks. This is a rather comforting check of the analysis we pursued. The modal shape of higher frequency bands are characterized by vibrating and rotating blocks linked by string segments which assume the modal shape of a string of length ℓ_1, whose

fundamental frequency coincides the lower frequency limit of each band. Also notice that as frequency increases the bandwidth of each group of modes decreases.

Table 2.1

String Modal Resonant Frequencies (Hz), Determined by Eq.(2.11)

Band 1:	222	225	231	241	253	267	282	295	306	313
Band 2:	840	846	862	886	917	952	989	1026	1057	1079
Band 3:	1525	1547	1577	1610	1645	1677	1704	1725	1738	1740
Band 4:	2999	3006	3016	3030	3044	3058	3071	3081	3087	3090
Band 5:	4485	4489	4496	4504	4513	4522	4531	4537	4541	4543

Now we return to the two-dimensional membrane. The modes of the membrane are those of the above-analyzed string coupled with those of a string of length ℓ_3, the width of the membrane, i.e., (k_1,k_3) where k_1,k_3 are respectively wave vectors of the abovementioned string systems. This is best shown in Figure (2.3). Note that $k^2 = k_1^2 + k_3^2 = \omega^2\sigma/T$, and that $f = 2\pi k C_m$, where $C_m = \sqrt{T_m/\sigma}$ is independent of frequency, i.e., f varies linearly with k. Since in k-space the distance from origin to mode (k_1,k_3) is just k, we can easily transform modes from $\vec{k}$-space to frequency domain. First, we use a circle centering at the origin to pass the mode concerned in two-dimensional $\vec{k}$-space and cross the k-scale at k_p which, after multiplied by $2\pi C_m$, is just the resonant frequency of that mode (Figure 2.3).

III. THE RADIATED POWER

A high frequency, the stiffeners on the membrane act as rigid barriers. This explains why the $\vec{k}$-space picture of the membrane-stiffeners system looks much like that of an individual membrane bay.

In evaluating the radiated power of this system, we made two assumptions:

1. The radiation contributions from different membrane units are statistically uncorrelated.
2. Each membrane unit radiates as if it were mounted in an infinite rigid baffle.

These two assumptions need discussion. The first one is justified because the exciting wall-pressure field is not correlated between bays (cf. Section V).

Now let us consider the following case: A membrane is excited on one side by a pressure field, P, and is mounted in an array of membranes of the same size. The acoustic power radiated into the other side of the membrane includes the direct contribution, $\langle p^2 \rangle$, from the excited membrane plus the back reaction, $\langle p_r^2 \rangle$, from the rest of the membranes excited by p. Let σ_{rad} be the radiation coefficient, and Z the total damping, i.e., both mechanical and radiation, of the membrane. If v is the velocity field of the membrane, then $\langle v^2 \rangle \sim \langle P^2 \rangle / |Z|^2$. Also, we know $\langle p^2 \rangle / \rho c \sim \pi_{rad} \sim \sigma_{rad} \langle v^2 \rangle$ where π_{rad} is the acoustic power radiated directly from the membrane. Thus, $\langle p^2 \rangle \sim \langle P^2 \rangle \rho c \sigma_{rad} / |Z|^2$. In general, $\langle p^2 \rangle << \langle P^2 \rangle$. The same argument leads us to the conclusion that $\langle p_r^2 \rangle << \langle p^2 \rangle$. And this justifies assumption 2 stated above.

After the appropriateness of these two assumptions, we can consider each bay as an independent radiator, and further approximate each radiator as a rectangular membrane unit of length ℓ_1 in the direction of mean flow and of width

ℓ_3 inserted in a rigid baffle. The acoustic radiation into the side away from the flow is considered here. The analysis given in this and the following two sections is a repeat of Davies'[4] work on rectangular plates, and is being applied to each bay of our membrane and stiffeners system at high frequency.

We choose Cartesian Coordinates with x_1, x_3 in the directions of ℓ_1 and ℓ_3 respectively, and x_2 normal to the membrane, but away from the flow side. The equation of motion for membrane displacement $y(\vec{x},t)$ driven by a wall pressure, $p(\vec{x},t)$, is

$$T\nabla^2 y + m\beta \frac{\partial y}{\partial t} + m \frac{\partial^2 y}{\partial t^2} = -p(\vec{x},t) + P(\vec{x},x_2=0,t) \ , \qquad (3.1)$$

where T is the tension of the membrane, m is the area density of the membrane, $\beta = \eta_s|\omega|$ accounts for mechanical damping of the membrane through a linear dependence on velocity, η_s is the loss factor, and $P(\vec{x},x_2,t)$ is the acoustic pressure generated by the motion of the membrane.

At the interface $x_2 = 0$, the boundary condition is

$$\frac{\partial P}{\partial x_2} = -\rho \frac{\partial v}{\partial t} \ , \qquad (3.2)$$

where ρ is the fluid density, and $v(\vec{x},t) = \partial y/\partial t$. The displacement y vanishes at the edge of the bay.

The transverse velocity field of the membrane can be expanded in terms of orthogonal characteristic functions (the <u>in vacuo</u> normal modes). The frequency Fourier transform of membrane velocity is written

$$v(\vec{x},\omega) = \int_{-\infty}^{\infty} v(\vec{x},t) e^{i\omega t}\, dt = \sum_{m,n=1}^{\infty} v_{mn}(\omega)\ \psi_{mn}(\vec{x})$$

where $\psi_{mn}(\vec{x}) = (2/\sqrt{A}) \sin k_m x_1 \sin k_n x_3$. Here $k_m = m\pi/\ell_1$, $k_n = n\pi/\ell_3$, and $A = \ell_1\ell_3$ is the area of the membrane unit. The modal equation obtained from Eq.(3.1) has the form

$$(-T\, k_{mn}^2 + i\omega^2 m\eta_s \operatorname{sgn} \omega - \omega^2 m)\, v_{mn}(\omega) = + i\omega p_{mn}(\omega) - i\omega P_{mn}(\omega) \quad , \tag{3.3}$$

where $k_{mn}^2 = k_m^2 + k_n^2$, and p_{mn} and P_{mn} are defined by

$$p_{mn}(\omega) = \int_A p(\vec{x},\omega)\, \psi_{mn}(\vec{x})\, d\vec{x},$$

$$P_{mn}(\omega) = \int_A P(\vec{x},\omega)\, \psi_{mn}(\vec{x})\, d\vec{x} \quad .$$

The wavenumber-frequency Fourier transforms of acoustic pressure and membrane velocity are connected by using Eq.(3.2), together with the wave equation for the acoustic medium. Thus,

$$P(k,x_2,\omega) = Z(\vec{k},\omega)\, v\, (\vec{k},\omega) \exp[ix_2(k_o^2-k^2)^{1/2}] \tag{3.4}$$

where $\vec{k}$ is the wavenumber vector on the membrane, $Z(\vec{k},\omega)$ is the radiation impedance defined by

$$Z(\vec{k},\omega) = \rho_o C_o (1 - k^2/k_o^2)^{-1/2} \quad ,$$

where $k = |\vec{k}|$, and $k_o = \omega/C_o$, C_o being the wave velocity in the acoustic medium.

Now $P_{mn}(\omega)$ can be written in the form

$$P_{mn}(\omega) = \frac{1}{(2\pi)^2} \sum_{qp} V_{qp}(\omega) \int_{-\infty}^{\infty} \int_{-\infty}^{\infty} Z(\vec{k},\omega)\, S_{qp}\, (\vec{k})\, S_{mn}^*(\vec{k})\, d\vec{k} \quad , \tag{3.5}$$

where $S_{mn}(\vec{k}) = \int_A \psi_{mn}(\vec{x}) e^{i\vec{k}\cdot\vec{x}} d\vec{x}$

and the asterisk denotes a complex conjugate.

We consider here a system where the response is primarily due to resonant modes and are thus interested in the value of P_{mn} only at the resonant frequency of the (m,n)

modes. If the resonant frequencies are widely separated in frequency, (m,n) is the only effective term in the summation. $P_{mn}(\omega)$ thus can be approximated by one term

$$P_{mn}(\omega) = \rho_o C_o \, v_{mn}(\omega)(\sigma_{mn} + i\chi_{mn})$$

with

$$\sigma_{mn} + i\chi_{mn} = \frac{1}{(2\pi)^2 \rho_o C_o} \int Z(\vec{k},\omega) |S_{mn}(\vec{k})|^2 \, d\vec{k} \qquad (3.6)$$

With this approximation, the modal velocity is given in terms of the modal wall pressure p_{mn} by the equation

$$v_{mn}(\omega) = Y_{mn}(\omega) \; p_{mn}(\omega) \quad , \qquad (3.7)$$

From Eq.(3.3), Y_{mn} is obtained,

$$Y_{mn}(\omega) = i\omega\{(-Tk_{mn}^2 - \omega^2 m - \omega\rho_o C_o \chi_{mn}) + i(\omega^2 m\eta_s \; \text{sgn}\; \omega + \omega\rho_o C_o \sigma_{mn})\} \qquad (3.8)$$

It is shown in Section II that the virtual mass term involving χ_{mn} is. in general, negligible for acoustically slow modes if the acoustic medium is air.

The wavenumber-frequency transform of acoustic pressure can now be written in the form

$$P(k,x_2,\omega) = Z(\vec{k},\omega) \sum_{m,n} Y_{mn}(\omega) p_{mn}(\omega) S_{mn}(\vec{k}) \exp[ix_2(k_o^2 - k^2)^{1/2}]$$

And $P(\vec{x},x_2,\omega)$ can be obtained from the inverse transform. Thus, the spectral density of the power-radiated $\pi(\omega)$, is written

$$\pi(\omega) = \int_A E[P(\vec{x},o,\omega) \; v^*(\vec{x},\omega)] \, d\vec{x} \quad , \qquad (3.9)$$

where it is understood that the real part of the integral is taken as the acoustic radiation.

Substitute the expressions of panel velocity and acoustic pressure into Eq.(3.9) and we have the spectral density

written in the form

$$\pi(\omega) = \frac{1}{(2\pi)^4} \sum_{m,n} \sum_{q,p} \int_{-\infty}^{\infty} Z(\vec{k},\omega) S_{mn}(\vec{k}) S^*_{qp}(\vec{k}) d\vec{k}$$

$$\times Y_{mn}(\omega) Y^*_{qp}(\omega) \int_{-\infty}^{\infty} \phi(\vec{k},\omega) S_{mn}(\vec{k}) S^*_{qp}(\vec{k}) d\vec{k} \quad ,$$

where $\phi(\vec{k},\omega)$ is the wavenumber-frequency transform of the wall-pressure cross-correlation.

Using Dyer's criteria,[7] we can reduce the summations of Eq.(1.10) to a single infinite summation. Essentially, it is assumed that $\phi(\vec{k},\omega)$ is constant in $\vec{k}$. The cross terms in Eq.(3.10) thus vanish because of the orthogonality of the modes.

$$\pi(\omega) = \rho_o C_o \sum_{m,n} \phi_{mn}(\omega) |Y_{mn}(\omega)|^2 \sigma_{mn}(\omega) \quad , \tag{3.11}$$

where

$$\phi_{mn}(\omega) = \frac{1}{(2\pi)^2} \int \phi(\vec{k},\omega) |S_{mn}(\vec{k})|^2 \, d\vec{k} \tag{3.12}$$

is the modal wall-pressure spectral density.

Again, since we are treating a highly resonant system, the radiated power in a narrow frequency band is dominated by radiation from those membrane modes that have resonant frequencies lying in the band. Eq.(3.11) can then be integrated over the narrow band $\Delta\omega$ centered on ω_o to give

$$\pi(\omega_o)\Delta\omega = \rho_o C_o \sum_{m,n} \sigma_{mn}(\omega_o) \phi_{mn}(\omega_o) \int_{\omega_o - \Delta\omega/2}^{\omega_o + \Delta\omega/2} |Y_{mn}(\omega)|^2 \, d\omega \quad ,$$

where the summation now includes only those modes resonant in the $\Delta\omega$ band. The integral is evaluated by writing $\omega = \omega_{mn}(1+\gamma) \approx \omega_o(1+\gamma)$, where $\gamma << 1$ for frequencies in the $\Delta\omega$ band. Also, let us define $\eta_{mn} = \eta_s + (\rho_o C_c/\omega_o m_p)\sigma_{mn}$, a loss factor including both mechanical and acoustic losses.

Further, we assume $\eta_{mn} << \Delta\omega/2\omega_o << 1$. Thus,

$$\int_{\omega_o-\Delta\omega/2}^{\omega_o+\Delta\omega/2} |Y_{mn}(\omega)|^2 \, d\omega \approx 2 \int_0^{\Delta\omega/2\omega_o} \omega_o |Y_{mn}|^2 d\gamma \approx \frac{\pi}{2\eta_{mn}\omega_o m^2}$$

And now,

$$\pi(\omega) = \rho_o c_o \frac{\pi}{2\omega m^2} \left(\sum_{m,n} \frac{\sigma_{mn}(\omega)\,\phi_{mn}(\omega)}{\eta_{mn}} \right) / \Delta\omega \qquad (3.13)$$

In the present experiment, it was only possible to measure total loss factors in 1/3-octave frequency bands. Thus, it is reasonable to assume a constant η_{mn} for the frequency band. Also note that ϕ_{mn}/η_{mn} is proportional to the modal energy. An assumption of statistical energy analysis (SEA) is that the power flow from the membrane to the acoustic medium can be estimated by treating the modal energies of all modes in the frequency band as equal. Then ϕ_{mn}/η_{mn} can be taken outside the summation in Eq.(3.13) and the expression rewritten in the form

$$\pi(\omega) = \rho_o c_o (\pi/2\eta\omega m^2)\; n_s \langle\sigma_{mn}\rangle\langle\phi_{mn}\rangle \,, \qquad (3.14)$$

where $\langle\cdots\rangle$ represents an average value over resonant modes in the $\Delta\omega$ band and n_s is the frequency mode density.

IV. MODAL RADIATION COEFFICIENTS

Eq.(3.6) can be written in the form

$$\sigma_{mn} + i\chi_{mn} = \frac{16\, k_o}{(2\pi)^2 A} \int_0^\infty \int_0^\infty \frac{I_1(k_1) I_3(k_3)}{(k_o^2-k_1^2-k_3^2)^{1/2}} \, dk_1 dk_3 \,, \qquad (4.1)$$

where

$$I_1 = \frac{2}{k_m^2} \frac{2[1-(-1)^m \cos k_1 \ell_1]}{(1-k_1^2/k_m^2)^2} \,, \qquad (4.2)$$

and I_3 has a similar form. The membrane studied in the

present report has a wave speed of about 1/3 the acoustic speed in the air. Thus, the functions here are evaluated only for acoustically slow modes; in fact, the restriction $k_{mn} > 2k_o$ is imposed. Therefore, the integral for χ_{mn} always includes the point $k_1 = k_m$, $k_3 = k_n$. Then, both I_1 and I_3 can be approximated by delta functions (see Reference 6).

$$I_1 = \frac{\pi \ell_1}{2} \delta(k_1 - k_m)$$

The integration now yields $\chi_{mn} \simeq k_o/k_{mn}$. The virtual mass term in Eq.(3.8) is

$$\omega^2 m\left(\frac{\rho_o c_o}{\omega m} \chi_{mn}\right) \simeq \omega^2 m\left(\frac{\rho_o}{m} \frac{1}{k_{mn}}\right) < \omega^2 m(0.05) \quad .$$

where density of air, ρ_o, is 1.29 Kg/m^3, surface density of the membrane, m, is 0.292 Kg/m^2, and k_{mn} is given its smallest value in the experiment reported here, 80 1/m (at 1500 Hz). The virtual mass term can thus be neglected.

Approximations to the modal radiation coefficients σ_{mn} for various frequency regimes have been given by Maidanik and Davies. The results are applied here to our cases. First, consider cases where $k_m > 2k_o$.

(a) n = 1 or 2

Approximate results are:

$$\sigma_{m1} = \frac{1}{(2\pi)^2} \frac{32\pi}{A} \frac{k_o \ell_3}{k_m^2 \pi^2} \left[1 + \frac{\sin(k_o \ell_3/2.4)}{k_o \ell_3/2.4} - (-1)^m \frac{\sin k_o \ell_1}{k_o \ell_1}\right.$$

$$\left. - (-1)^m \frac{\sin k_o [\ell_3^2/(2.4)^2 + \ell_1^2]^{1/2}}{k_o [\ell_3^2/(2.4)^2 + \ell_1^2]^{1/2}}\right) ,$$

$$\sigma_{m2} = \frac{1}{(2\rho)^2} \frac{32\pi}{A} \frac{k_o \ell_3^2}{k_m^2} (0.068) \left\{1 - \frac{\sin(k_o \ell_3/1.7)}{k_o \ell_3/1.7} - (-1)^m \frac{\sin k_o \ell_1}{k_o \ell_1}\right.$$

$$\left. + (-1)^m \frac{\sin k_o [\ell_3^2/(1.7)^2 + \ell_1^2]^{1/2}}{k_o [\ell_3^2/(1.7)^2 + \ell_1^2]^{1/2}}\right) \qquad (4.3)$$

(b) $k_n < k_o$ (m,n>2), edge modes

$$\sigma_{mn} = \frac{1}{(2\pi)^2} \frac{8\pi^2}{A} \frac{k_o \ell_3}{k_m^2} \left(1 - (-1)^m J_o[\ell_1 (k_o^2 - k_n^2)^{1/2}]\right) \qquad (4.4)$$

(c) $k_o < k_n < 2k_o$ (m,n>2), transition region between edge and corner modes

$$\sigma_{mn} = \frac{1}{(2\rho)^2} \frac{2\pi}{A} \frac{k_o}{k_m^2 k_n} \left[\ln\left(\frac{1 + k_o/k_n}{1 - k_o/k_n}\right) + \frac{2k_o/k_n}{(1 - k_o^2/k_n^2)}\right] \qquad (4.5)$$

(d) $k_n > 2k_o$ (m,n>2), corner modes

$$\sigma_{mn} = \frac{1}{(2\pi)^2} \frac{32\pi}{A} \frac{k_o^2}{k_m^2 k_n^2} \left(1 - (-1)^m \frac{\sin k_o \ell_1}{k_o \ell_1} - (-1)^n \frac{\sin k_o \ell_3}{k_o \ell_3}\right.$$

$$\left. + (-1)^{m+n} \frac{\sin k_o (\ell_1^2 - \ell_3^2)^{1/2}}{k_o (\ell_1^2 + \ell_3^2)^{1/2}}\right) \qquad (4.6)$$

Similar expressions exist for $k_m > 2k_o$ cases.

The average value of Eq.(4.6) can be taken as representative of the radiation coefficient for small values of $k_o \ell_1$ and $k_o \ell_3$, and is written

$$\sigma_{mn} = \frac{1}{(2\pi)^2} \frac{32\pi}{A} \frac{k_o^2}{k_m^2 k_n^2}, \qquad (4.7)$$

Inspection of Figure (4.1) shows that this typical value is valid approximately for all modes such that $k_o \ell_1$ and $k_o \ell_3 < 3\pi$. The total average value of the radiation coefficients

of the (corner) modes resonant in the $\Delta\omega$ band is then obtained, for $k_o\ell_1$, $k_o\ell_3 < 3\pi$, as

$$\langle\sigma_{mn}\rangle = \frac{2}{\rho k_p} \int_{\frac{\pi}{2k_p\ell_3}}^{\frac{\pi}{2} - \frac{\pi}{2k_p\ell_1}} \sigma_{mn}\, k_p\, d\theta = \frac{32}{\pi^3 A_p} \frac{k_o^2}{k_p^3} (\ell_1 + \ell_3) \qquad (4.8)$$

For either or both of $k_o\ell_1$ or $k_o\ell_3 \geq 3\pi$, some modes contribute as edge modes. The average value is then obtained as

$$\langle\sigma_{mn}\rangle = \frac{32}{\pi A} \frac{k_o}{k_p^3} + \frac{4}{\pi A} \frac{k_o^2}{k_p^3} (\ell_1 + \ell_3) \quad . \qquad (4.9)$$

V. MODAL WALL-PRESSURE SPECTRUM

Assuming Corcos's model for the wall-pressure correlation function,

$$\phi(\vec{r},\omega) = \phi(\omega) \exp\left(- \frac{|\omega r_1|}{\alpha_1 U_c} - \frac{|\omega r_3|}{\alpha_3 U_c} - \frac{i\omega r_1}{U_c}\right) ,$$

where U_c is the convection velocity, and has a value of about $0.7U_\infty$, and $\phi(\omega)$ is the frequency spectral density, Blake[8] showed that $\alpha_1 = 8$ and $\alpha_3 = 1.1$, for the wind tunnel where the experiments reported here were done.

The correlation length in the x_1-direction is $\alpha_1 U_c/\omega$, according to the above Corcos's model. For frequency range higher than 1 kHz, and $U_\infty = 48$ m/sec, $\alpha_1 U_c/\omega$ is smaller than ℓ_1, the longitudinal dimension of one membrane unit. This justifies assumption 2 made in Section III. The radiation contributions from different membrane units are statistically uncorrelated.

It was shown by Davies[4] that Eq.(3.12) can be rewritten in the form,

$$\phi_{mn}(\omega) = 2\phi(\omega) \left(\frac{\beta_1}{(k_m-\omega/U_c)^2 + \beta_1^2} + \frac{\beta_1}{(k_m+\omega/U_c)^2 + \beta_1^2}\right)\left(\frac{\beta_3}{k_n^2 + \beta_3^2}\right) \tag{5.3}$$

where $\beta_1 = \omega/\alpha_1 U_c$ and $\beta_3 = \omega/\alpha_3 U_c$. Thus, the total average value of the modal wall-pressure spectral density over the resonant modes in a $\Delta\omega$ band is then in the form

$$\langle\phi_{mn}\rangle = \frac{2}{\pi k_p} \int_0^{\frac{\pi}{2}} \phi_{mn}(\omega)\ k_p d\Theta$$

$$= \phi(\omega)\ \frac{4\alpha_1\alpha_3}{\pi}\ \frac{U_c^2}{\omega^2}\ \int_0^{\pi/2} \left([1+\alpha_1^2(1-\gamma\cos\Theta)^2]^{-1} + [1+\alpha_1^2(1+\gamma\cos\Theta)^2]^{-1}\right)$$

$$x\ (1 + \alpha_3^2\ \gamma^2\ \sin^2\Theta)^{-1}\ d\Theta \tag{5.4}$$

where $\gamma = U_c k_p/\omega = U_c/C_p$.

Since $\gamma < 0.1$, the integral in Eq.(5.4) can be approximated as

$$\langle\phi_{mn}\rangle = \phi(\omega)\ \frac{4\alpha_3 U_c^2}{\alpha_1 \omega^2} \tag{5.5}$$

VI. EXPERIMENTAL RESULTS

Experimental Apparatus

A 28-inch diameter mylar (polyethylene terephlatate) bass drum head was uniformly tensioned on a bass drum frame. The uniformity of the tension was determined by exciting the circular mylar membrane acoustically from underneath with pure tones at its resonant frequencies. The resultant Chladni patterns were observed using a light dusting of fine sand to identify nodes.

With uniform tension achieved, a backing plate of 3/4-inch plywood was cemented to the lower surface of the mylar membrane. This backing plate contained a plexiglass-edged,

rectangular-shaped cutout which served to define the desired membrane. Again, acoustic excitation and sand were used to observe the Chladni patterns of the rectangular membrane. It was from these observations that modal resonant frequency response could be correlated to specific modes.

Then we cemented nine aluminum square bars periodically spaced onto the lower surface of the rectangular membrane. To avoid extreme local stresses due to the square shoulders of the stiffeners, the bars are tapered at the end. Also to allow heaving freedom of the bars on the membrane, there are small gaps between the bar-ends and the boundaries (plexiglass) of the membrane. The effects of these small gaps, e.g., scattering of waves in the membrane, are not clear at the moment. The membrane and stiffeners system had the following characteristics (Figure 6.1):

1. Membrane dimensions: $L_1 = 54.5$ cm, $L_3 = 11.5$ cm
2. Thickness: 8.5 mils
3. Surface density: $\sigma = 0.292$ Kg/m^2
4. Spacing of stiffeners: 4.59 cm
5. Stiffener dimensions: 10 cm x .933 cm x .933 cm

Before the rectangular membrane was stiffened, for an (m,n) mode, its resonant frequency $f_{m,n}$ and the membrane wave speed $C_{m,n}$ are related by Morse.[9]

$$f_{m,n} = \frac{1}{2} \cdot C_{m,n} \cdot \left(\frac{m}{L_1}\right)^2 + \left(\frac{n}{L_3}\right)^2 ,$$

where $C^2_{m,n} = T/\sigma_{total}$, and $\sigma_{total} = \sigma$ + added mass. At high frequencies, the modal added mass of a resonantly responding mode becomes vanishingly small, hence the value of $C_{m,n}$

approaches asymptotically the in vacuo membrane wave speed, C_i, which determines the membrane tension, T. Before stiffened by the aluminum bars, the C_i of this membrane was 137 m/sec (Figure 6.2).

Precaution was taken to eliminate most vibration of the backing plywood plate by attaching, with screws and cement, additional damping sheet lead 1/4-inch thick onto the plywood. The backed membrane, still held by the tensioning frame, was flush-mounted in the wind tunnel test section, forming the lower panel of the test section, with the longitudinal direction in the flow direction. The details of membrane mounting and test section are shown in Figures (6.3) and (6.4).

Total Damping of the Membrane and Stiffeners System

These measurements were performed in the following way. We first imposed a D.C. voltage to a shaker which would push upward against the membrane. Secondly, we fed the shaker, in addition, an A.C. signal of 1/3 octave white noise, but with the shaker tip in good contact with the membrane. Finally, we shut off the shaker so its tip was clear and away from the membrane and a fiberoptical displacement gauge flowed by 1/3 octave filter, preamplifier ard graph level recorder would observe and record the decay rate. The reverberation time, T_R, is the time needed for the level of a transient signal to decay 60 dB. Its relation with the loss factor η_t is $T_R = 2.2/f_o\eta_t$ where f_o is center frequency of the 1/3 octave band.

The loss factor for the system is plotted in Figure 6.5.

Displacement Measurements of Membrane

The turbulent boundary layer pressure fluctuations were created by the mean flow in the wind tunnel at speeds of 32 m/sec and 48 m/sec. Again we used the fiberoptical displacement gauge and graph level recorder to measure and record the vibration levels at many different positions of the membrane, in 1/3 octave bands. Finally, we averaged the data for each of the 1/3 octave bands. These values are shown in Figure 6.6.

Damping of Room

Standard techniques were employed in measuring the reverberation time, in 1/3 octave bands, of the reverberant chamber which housed the test section of the wind tunnel. Experimental results are presented in Figure 6.5.

Sound Pressure Level Measurements

The volume of the reverberant chamber is 893 ft^3. Again, standard techniques were used in these measurements. With the wind tunnel running at 32 m/sec and at 48 m/sec, three 1-inch B & K condenser microphones were used to measure simultaneously the sound levels at different positions, and these levels are averaged for each 1/3 octave band.

There is a minimum of 3 dB difference between the sound pressure level measured with the membrane system in place and the background noise level measured with a sand-loaded plywood box plugged onto the membrane system.

The measured and averaged sound pressure levels are shown in Figure 6.7.

VII. ESTIMATES ON RADIATED SOUND POWER LEVEL

(a) Based on Displacement Measurements

In a 1/3 octave band, whose lower and upper limiting frequencies are f_1 and f_2 respectively, the radiated sound power in watts is

$$\pi = \int_{f_1}^{f_2} R_{rad}\, V(f)\, df$$

where $R_{rad} = \rho_o C_o A \sigma_{rad}$ is the radiation resistance

A is the total vibrating area of the membrane

σ_{rad} is the radiation coefficient

$V(f) = (2\pi f)^2 D(f)$ is the spectral density of velocity and $D(f)$ is the displacement spectral density

We measured $D(f)$, and from previous analysis we computed σ_{rad}. From these data we obtained the radiated sound power level.

$$PWL = 120 + 10 \log_{10} \pi \text{ , dB } \underline{re}\ 10^{-12} \text{ watt}$$

The results are shown in Figure 7.1.

(b) Based on Sound Pressure Level Measurements

For a highly reverberant room, the sound power level is given by the following expression:

$$PWL = \overline{SPL} + 10 \log_{10} V + 10 \log_{10} D - 47.3$$

where $V = 893\ ft^3$ is the volume of the room

$D = 60/T_R$ is the decay rate in dB/sec

$\overline{SPL}$ is the average sound pressure level in the room

The radiated sound power levels calculated by this method are presented in Figure 7.1.

(c) Based on Wall Pressure Data

Wall pressure spectral density, $\phi(f)$, is readily available from Blake's report.[8] These data are shown in Figure 7.2. As shown in that figure, we approximated $\phi(f)$ of different frequency regions and of different wind tunnel speeds by several straight lines. The linear functions for these lines are listed in Table 7.1.

By inserting $\phi(f)$ into Eq.(3.14) and integrating over a 1/3 octave band, we obtained the radiated sound power levels as shown in Figure 7.1.

Table 7.1

Approximations for $\phi(f)$, the Wall Pressure Spectral Density

$U_\infty(\frac{m}{sec})$	$f \leq 2239^{Hz*}$	$f \geq 2239^{Hz*}$
32	$\phi(f)=.888\times10^{-3}-.229\times10^{-6}f$	$\phi(f)=.538\times10^{-3}-.712\times10^{-7}f$
48	$\phi(f)=.337\times10^{-2}-.105\times10^{-5}f$	$\phi(f)=.104\times10^{-2}$

Note: The unit for $\phi(f)$ is Kg^2/m^2sec^3.

*2239Hz is the upper limit frequency of the 33rd 1/3 octave band centering at 2000 Hz.

VIII. DISCUSSION

We sampled the vibratory response at many different positions on the periodically stiffened membrane. Figure 8.1 shows some typical examples. The samples show sharp and clear frequency band-pass characteristics, as the analysis in Section II pointed out.

We used three methods to estimate the radiated sound power levels at two different wind tunnel speeds, 32 m/sec and 48 m/sec. The first one was based on displacement mea-

surements, the second one on sound pressure level measurements, and the third one on wall pressure data. The experimentation showed good agreement among these three estimates.

In Figure 8.1, the first peak at about 250 Hz is due to the "heaving" modes or band #1, as predicted in Table 2.1. The second peak near 450 Hz is due to the "pitching" modes not covered by the analysis in Chapter II. This is easily understood by modeling our system as rectangular bars each resting on two springs at the ends of the bar, as shown in Figure 8.2. The ratio between the pitching and heaving resonant frequencies is about $\sqrt{3}$, and that is the ratio between the second and the first peaks, as discussed above.

We make the following study to see the reason why band #2, from 840 Hz to 1079 Hz, listed in Table 2.1, does not appear in the displacement spectrums. First, remember that the fundamental resonant frequency for a $\ell_1 \times \ell_3$ membrane unit is 1525 Hz, i.e., the lower frequency limit of band #3 (see Figure 2.3). Note that band #1 and band #2 are well below that frequency. This means, in the string and block model, that the strings between the blocks are nearly straight segments. For such a system, the cutoff frequency, f_o, is associated with $\lambda_o = \ell_1$ because, for $\lambda < \ell_1$, there will be cancellation of excitations. Secondly, note that heaving, $h_i \propto \Theta_i - \Theta_{i-1}$ and rolling, $\lambda_i \propto \Theta_i + \Theta_{i-1}$ (see Figure 8.3). Also note that, for high frequencies, the root mean squares of heaving and rolling, $\overline{h_i^2(\omega)}$ and $\overline{r_i^2(\omega)}$ are both proportional to $\overline{|\Theta_i(\omega)|^2} + \overline{|\Theta_{i-i}^2(\omega)|^2}$, since the cross-correlation of Θ_i and Θ_{i-1}, $\overline{\Theta_i(\omega)\Theta_{i-1}^*(\omega)} = 0$, which is true at least for $\lambda < \ell_1$. So we may conclude that

heaving and rolling modes both have the same cutoff frequency.

Next, we know that, for a frozen convecting turbulence, $k = 2\pi/\lambda = 2\pi f/U_c$ where $U_c = .7U_\infty$. The larger value of U_∞ is 48 m/sec in our experiments and $\ell_1 = 4.6$ cm. Thus, the cutoff frequency is $f_o = 0.7\ U_\infty/\ell_1 \simeq 700$ Hz. Finally, it is quite clear now that band #2, beyond the cutoff frequency, will not be excited by the turbulent boundary layer, while band #2, within the cutoff frequency, will be excited.

REFERENCES

1. Miles, J. W., "Vibrations of Beams on Many Supports," Journal of the Engineering Mechanics Division of the American Society of Civil Engineers, Vol. 82, No. EM1, Jan. 1956.

2. Lyon, R. and Maidanik, G., "Power Flow between Linearly Coupled Oscillators," JASA, 34, 623-639, 1962.

3. Leehey, P., "Trends in Boundary Layer Noise Research," AFOSR-UTIAS Symposium on Aerodynamic Noise, Toronto, 20-21 May 1968.

4. Davies, H., "Sound from Turbulent-Boundary-Layer-Excited Panels," JASA, 49, Mar. 1971, pp. 878-889.

5. Corcos, G., "Resolution of Pressure in Turbulence," JASA, 35, 1963, pp. 192-199.

6. Smith, P. and Lyon, R., "Sound and Structural Vibration," NASA, CR-160 (1965).

7. Dyer, I., "Response of Plates to a Decaying and Convecting Random Pressure Field," JASA, 31, 1959, pp. 922-928.

8. Blake, W., "Turbulent Boundary Layer Wall Pressure Fluctuations on Smooth and Rough Walls," MIT Rep. No. 70208-1, 1969.

9. Morse, P., Vibration and Sound, 2nd ed., McGraw-Hill Book Company, 1948, p. 180.

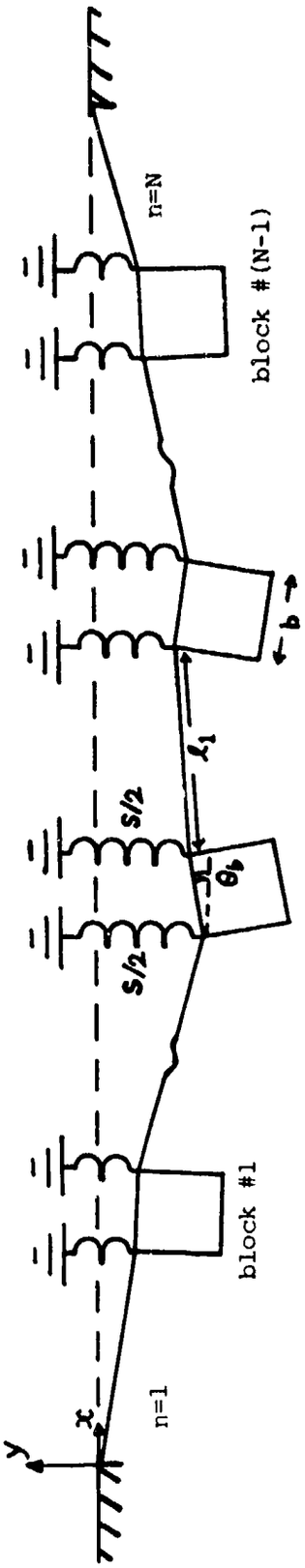

FIGURE 2.1 String and Block Model

$$z = \frac{(\alpha\beta-1)\sin\lambda + (\alpha+\beta)\cos\lambda}{\beta - \alpha}$$

FIGURUE 2.2 **z is plotted for the case where**
$\alpha = -.00306\omega + 6324/\omega$,
$\beta = -.00051\ \omega + 20708/\omega$, and
$\lambda = \frac{\ell_1}{C_m}\omega = .335 \times 10^{-3}\ \omega$

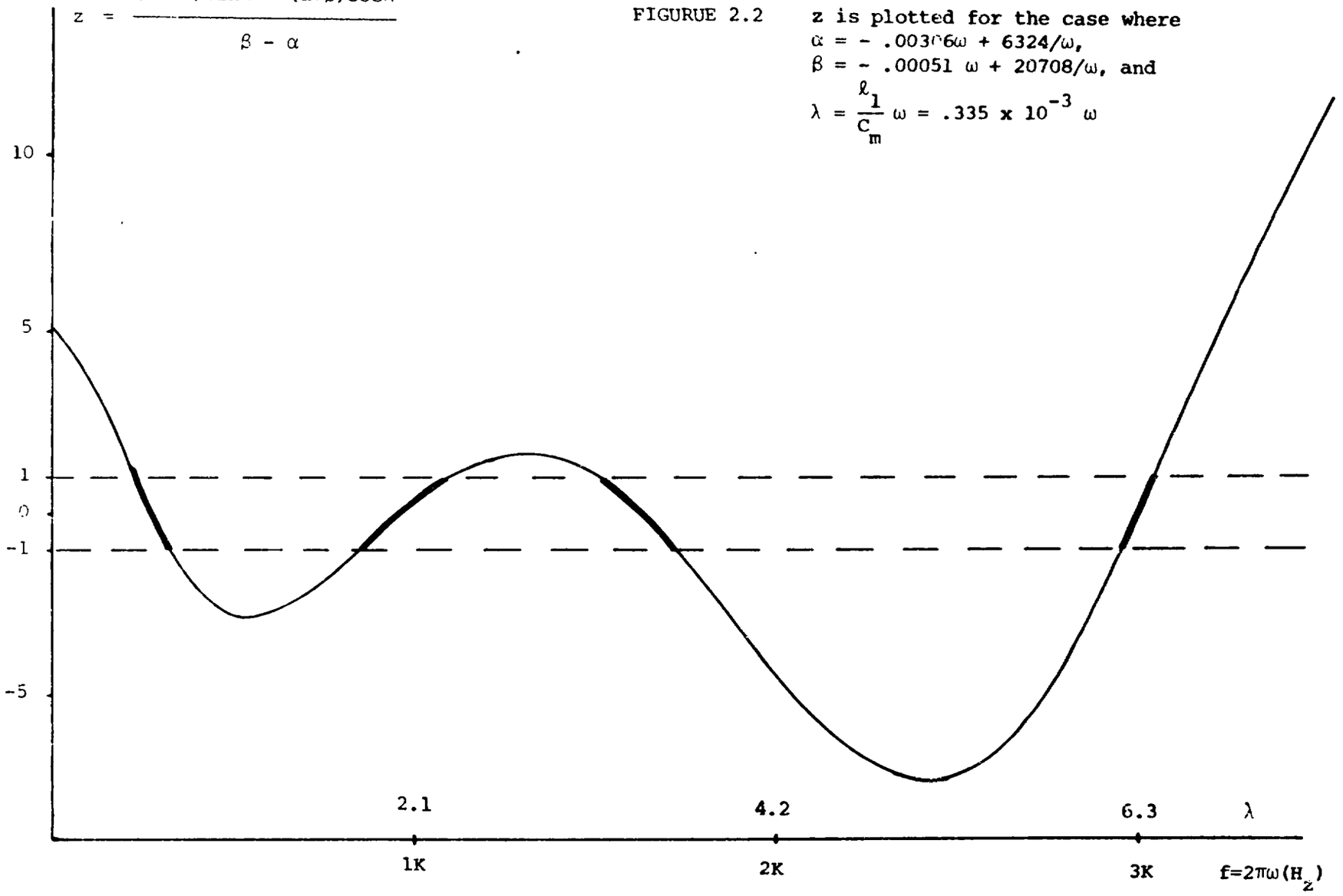

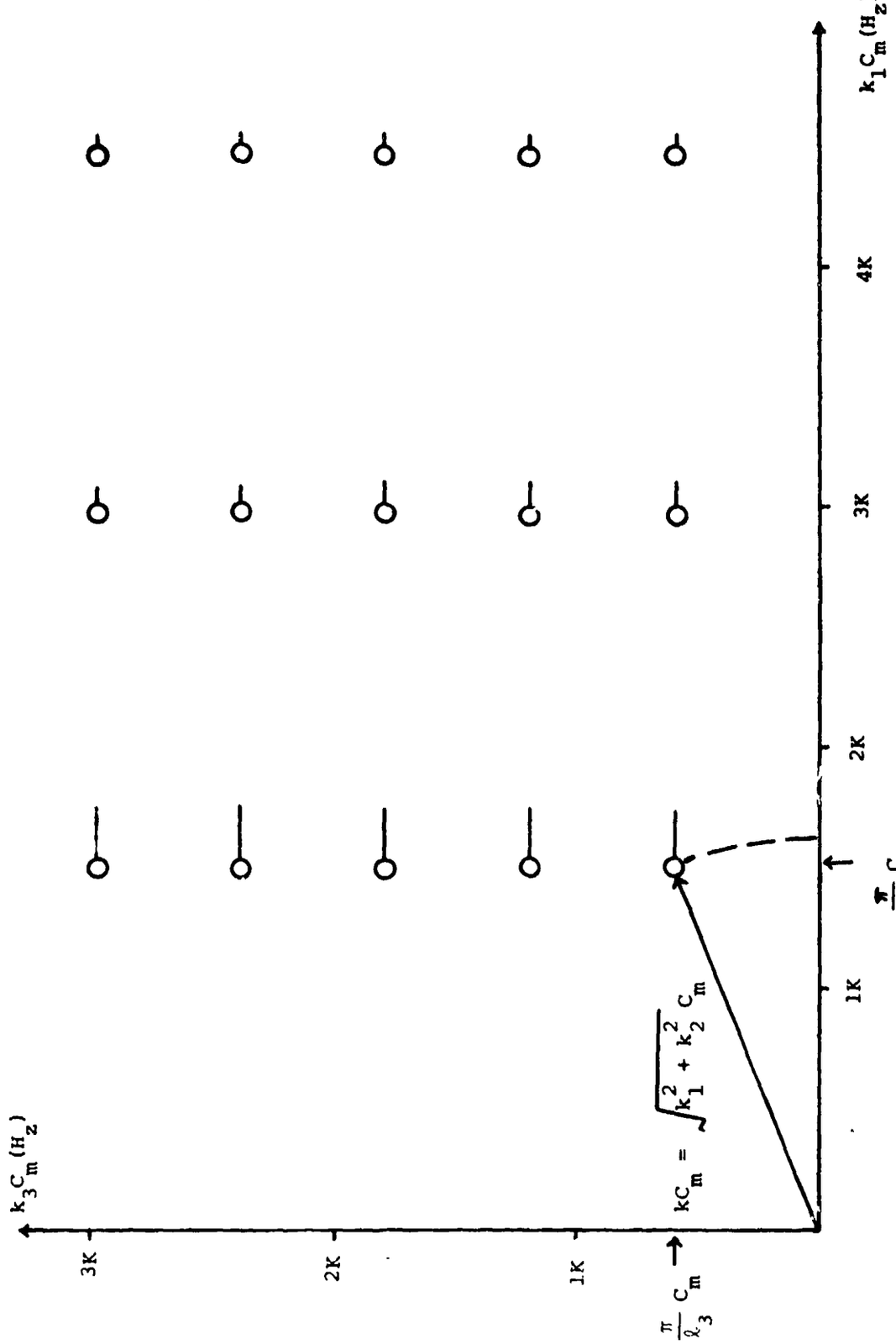

FIGURE 2.3 Resonant modes in $\vec{k}$-space (scaled by C_m). "o", for a ℓ_1 X ℓ_3 member unit. "-", for the periodically stiffened membrane (spacing between stiffeners is ℓ_1). Also please see Chapter VIII for further discussion.

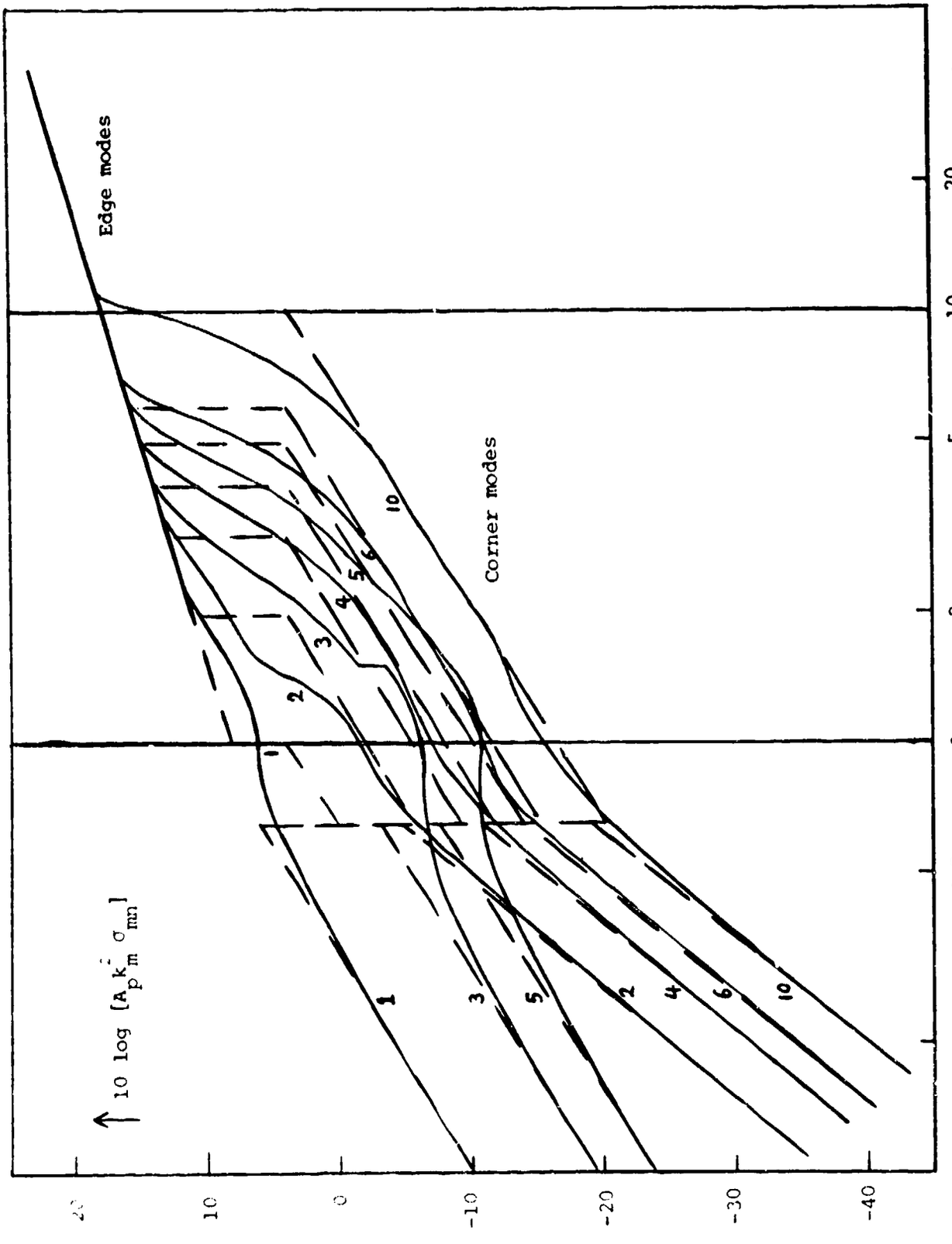

Figure 4. Values of the Radiation Coefficient σ_{mn} for large odd m and various n

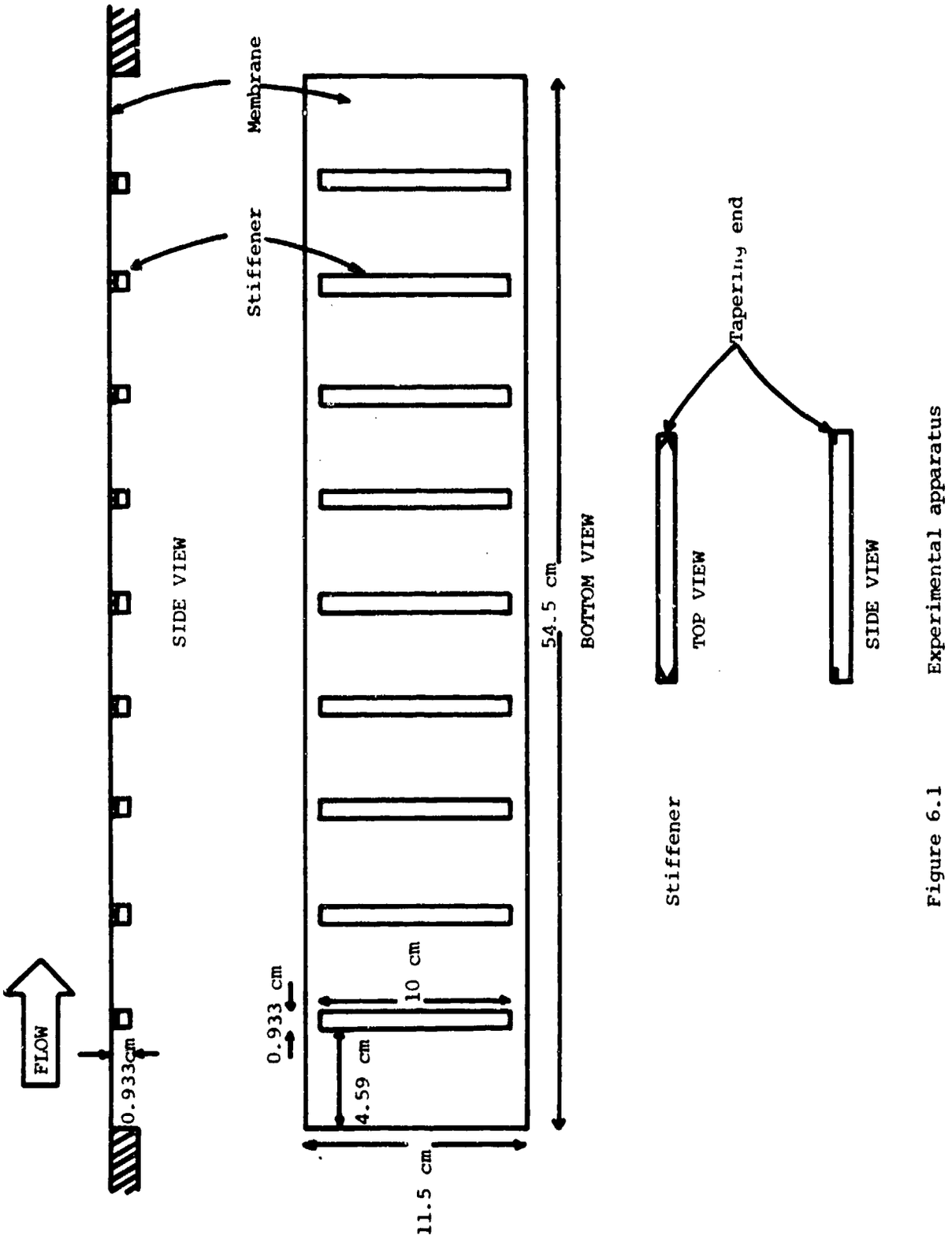

Figure 6.1 Experimental apparatus

Mode (N_x, N_y)	Frequency (Hz)	Wave speed C_{mn} (m/sec)
7, 1	1053	130.7
9, 1	1291	133.3
11, 1	1561	136.9
12, 1	1680	136.8
13, 1	1780	135.2
1, 3	1887	138.0
1, 4	2509	137.8
1, 5	3157	138.8

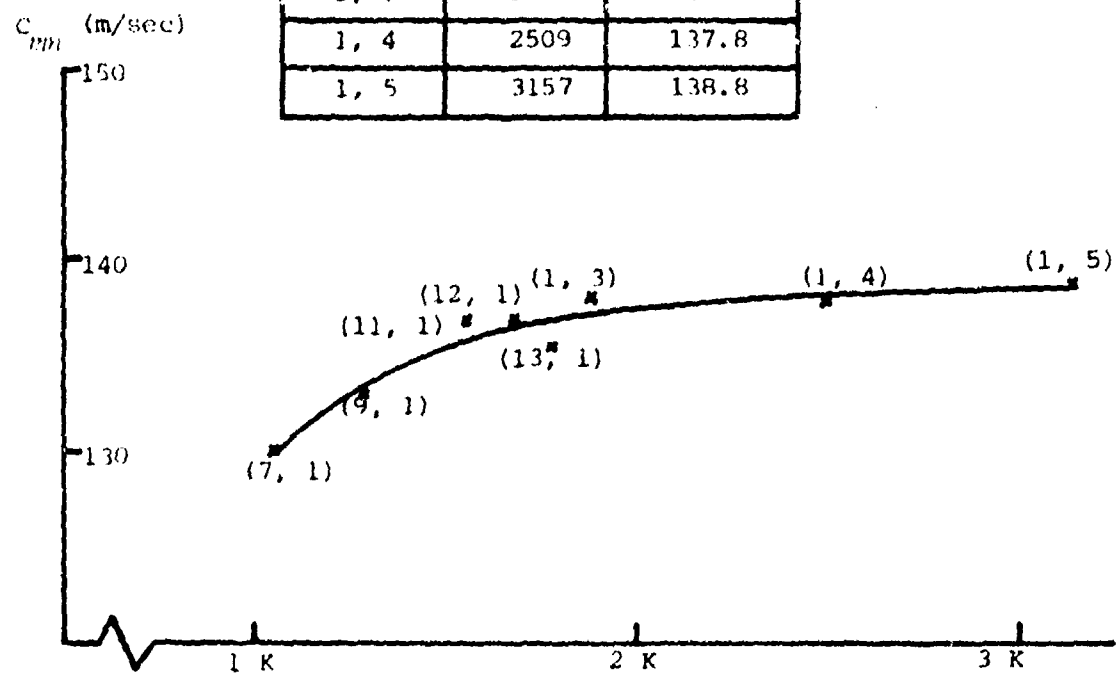

Figure 6.2 Membrane modal wave speeds $C_{m,n}$

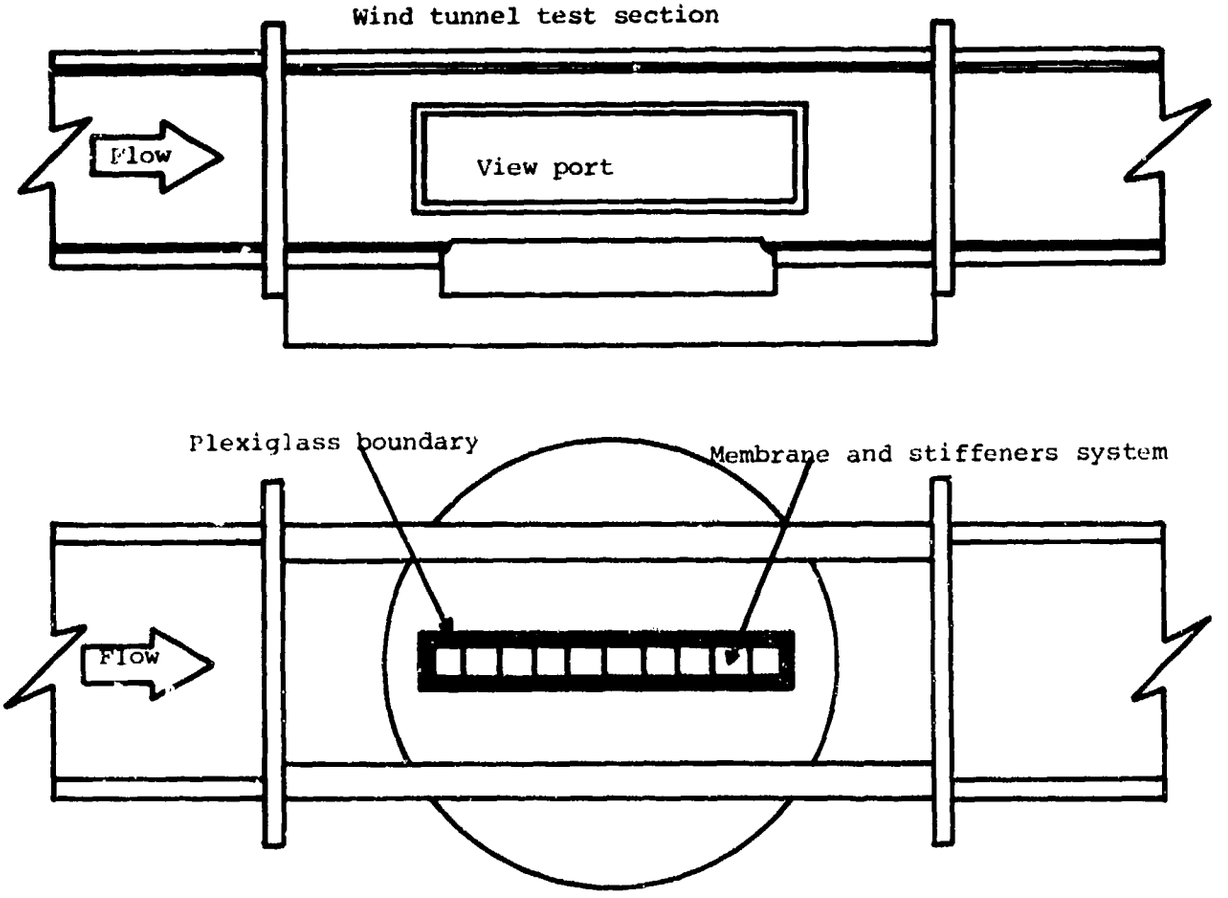

Figure 6.3 Membrane wind tunnel mounting detail

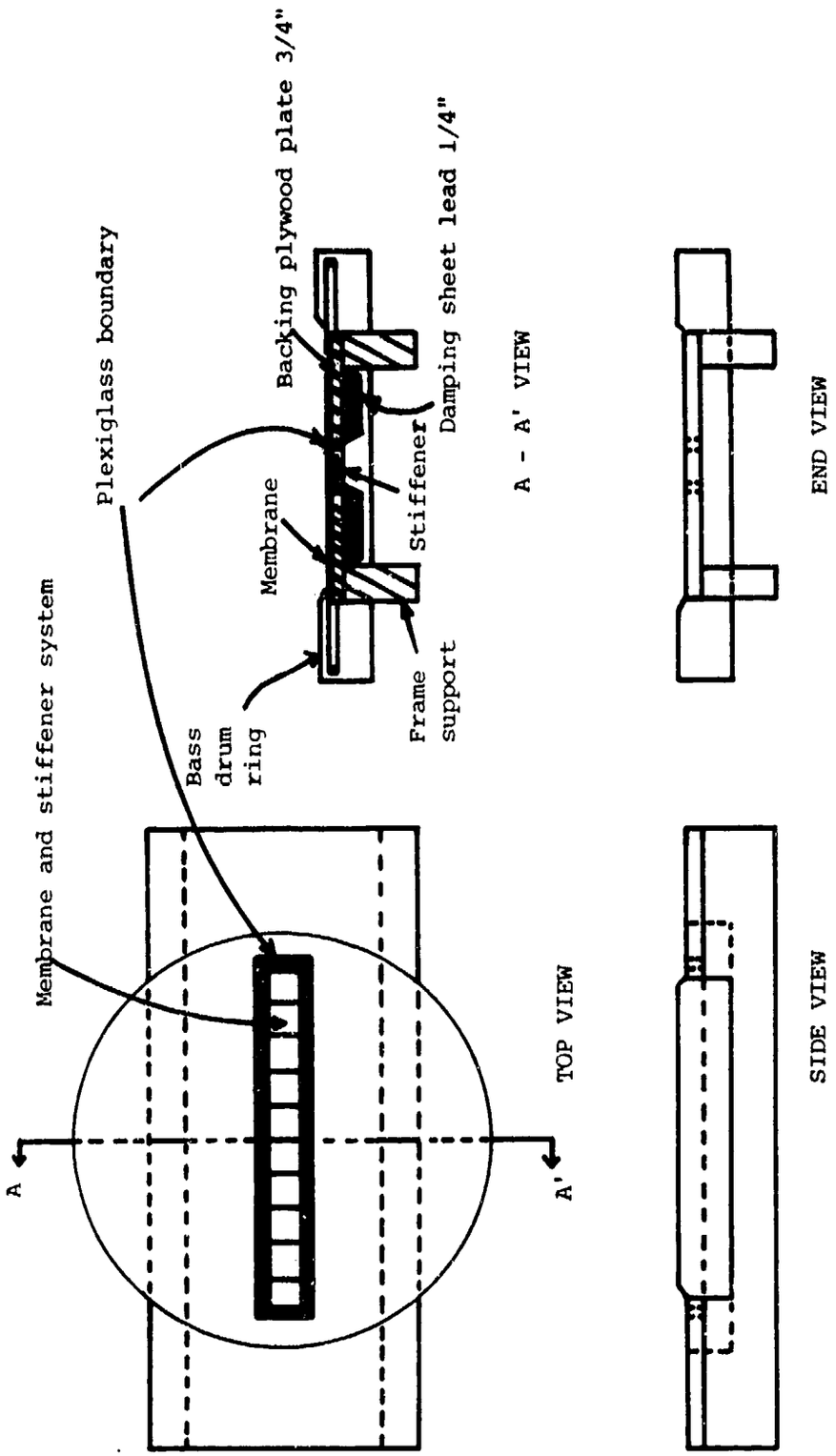

Figure 6.4 Membrane support mounting detail

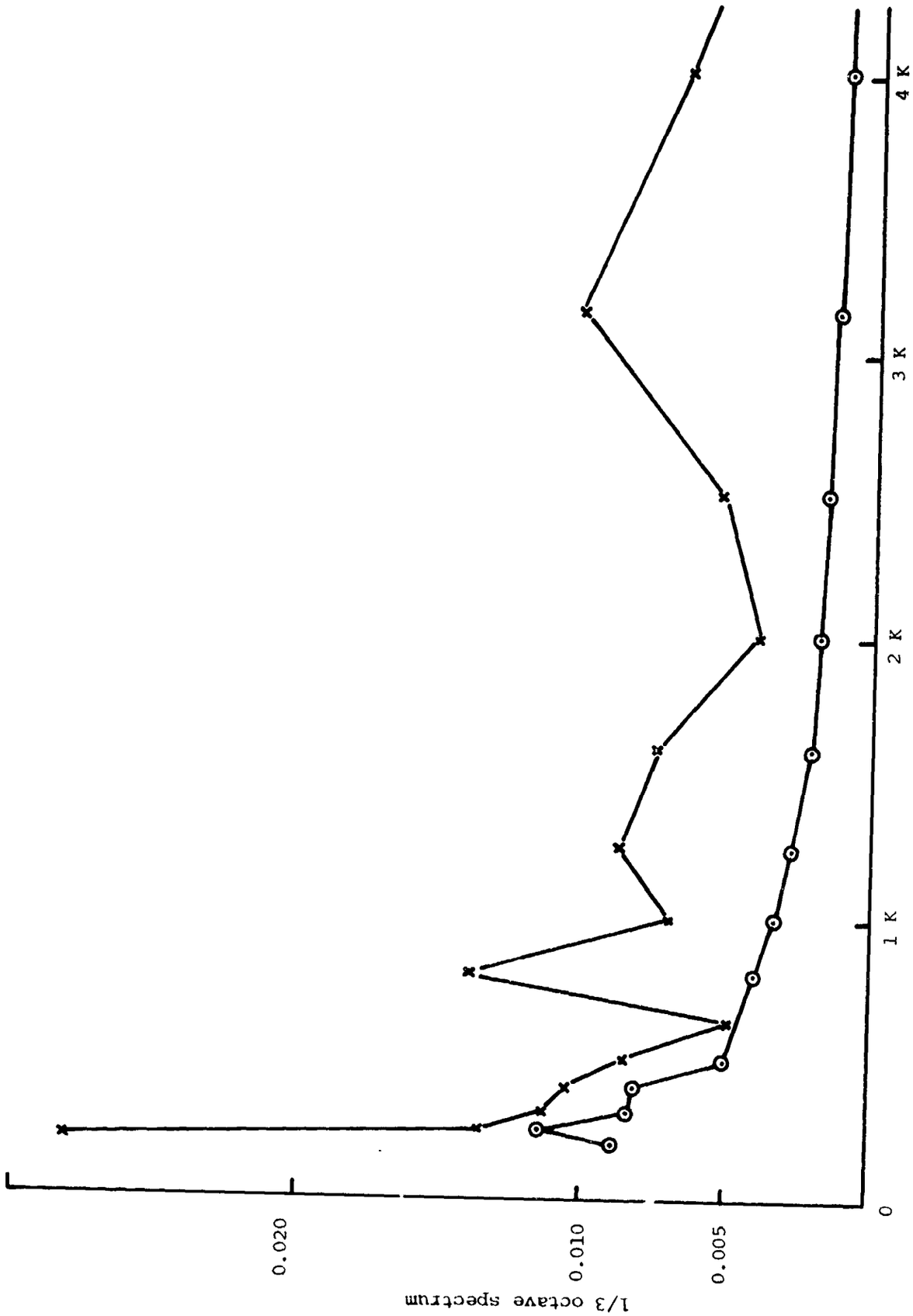

Figure 6.5 Loss factors. "x", total loss factor for membrane and stiffeners system. "o", loss factor for reverberant room, $\eta_t = 2.2/f_o T_R$, T_R is reverberation time.

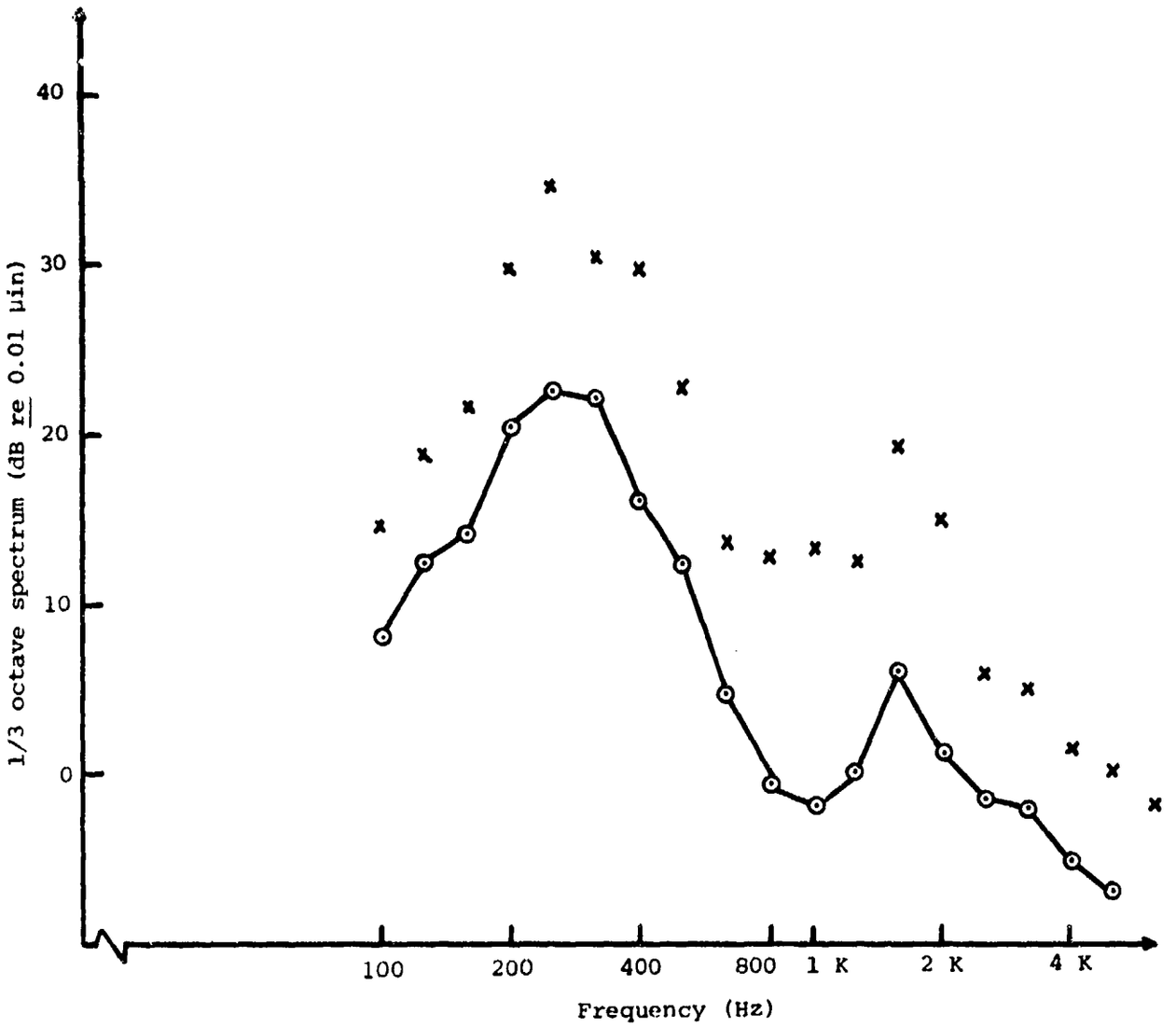

Figure 6.6 Displacement measurements of membrane excited by turbulent boundary layer pressure fluctations. "o", U_∞ = 32 m/sec; "x", U_∞ = 48 m/sec.

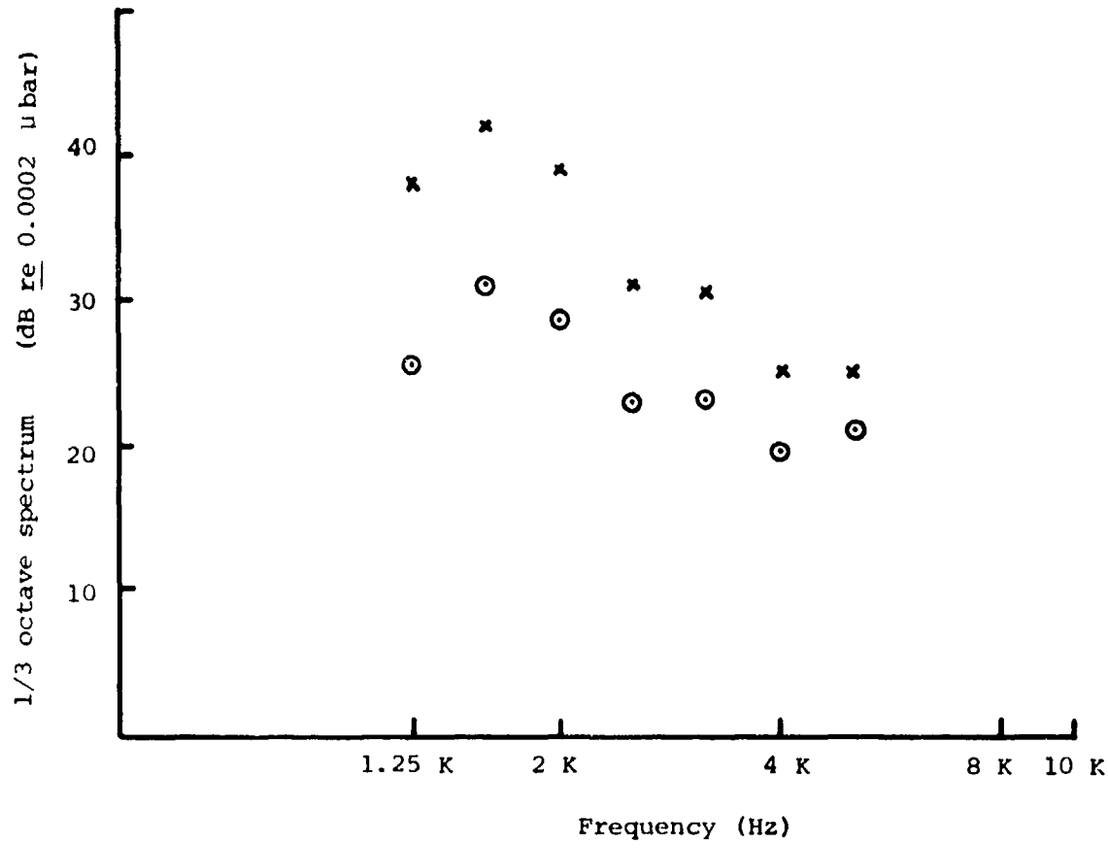

Figure 6.7 Averaged sound pressure level

"o", U_∞ = 32 m/sec. "x", U_∞ = 48 m/sec.

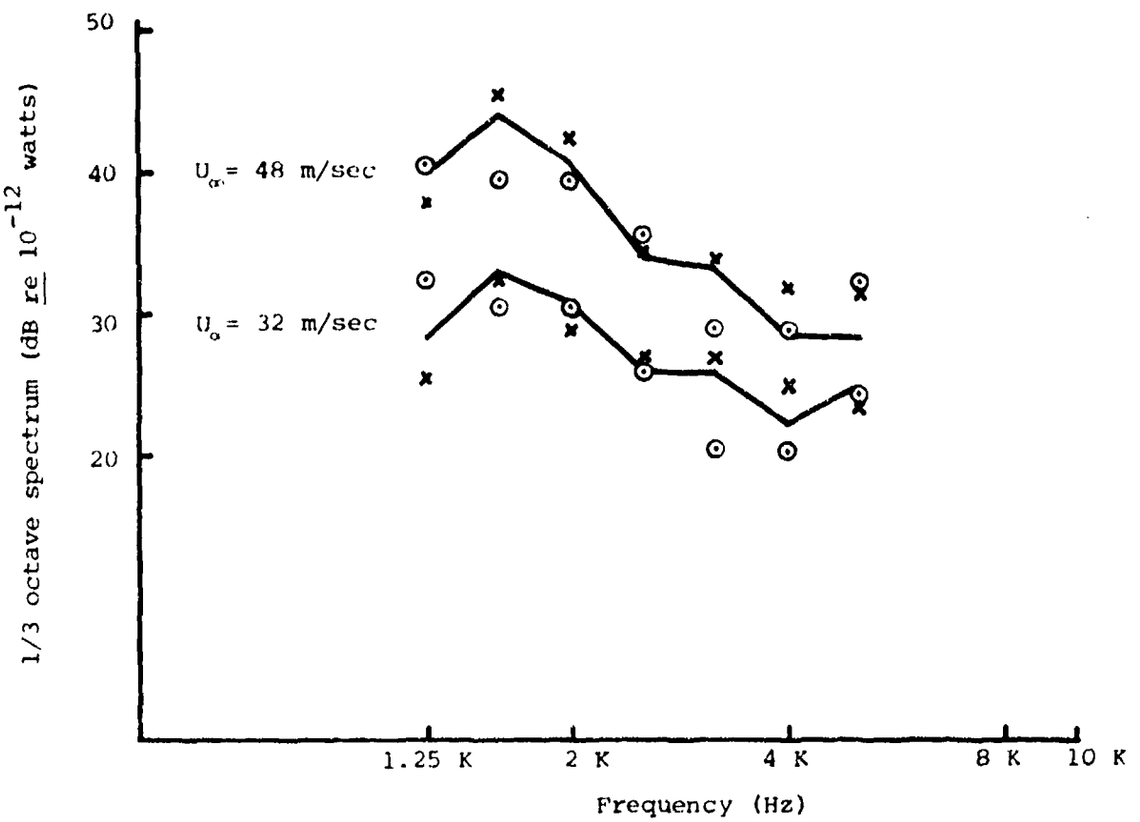

Figure 7.1 Radiated sound power level estimates.

"o", based on wall pressure data;

"x", based on displacement measurements;

"-", based on sound pressure level measurements.

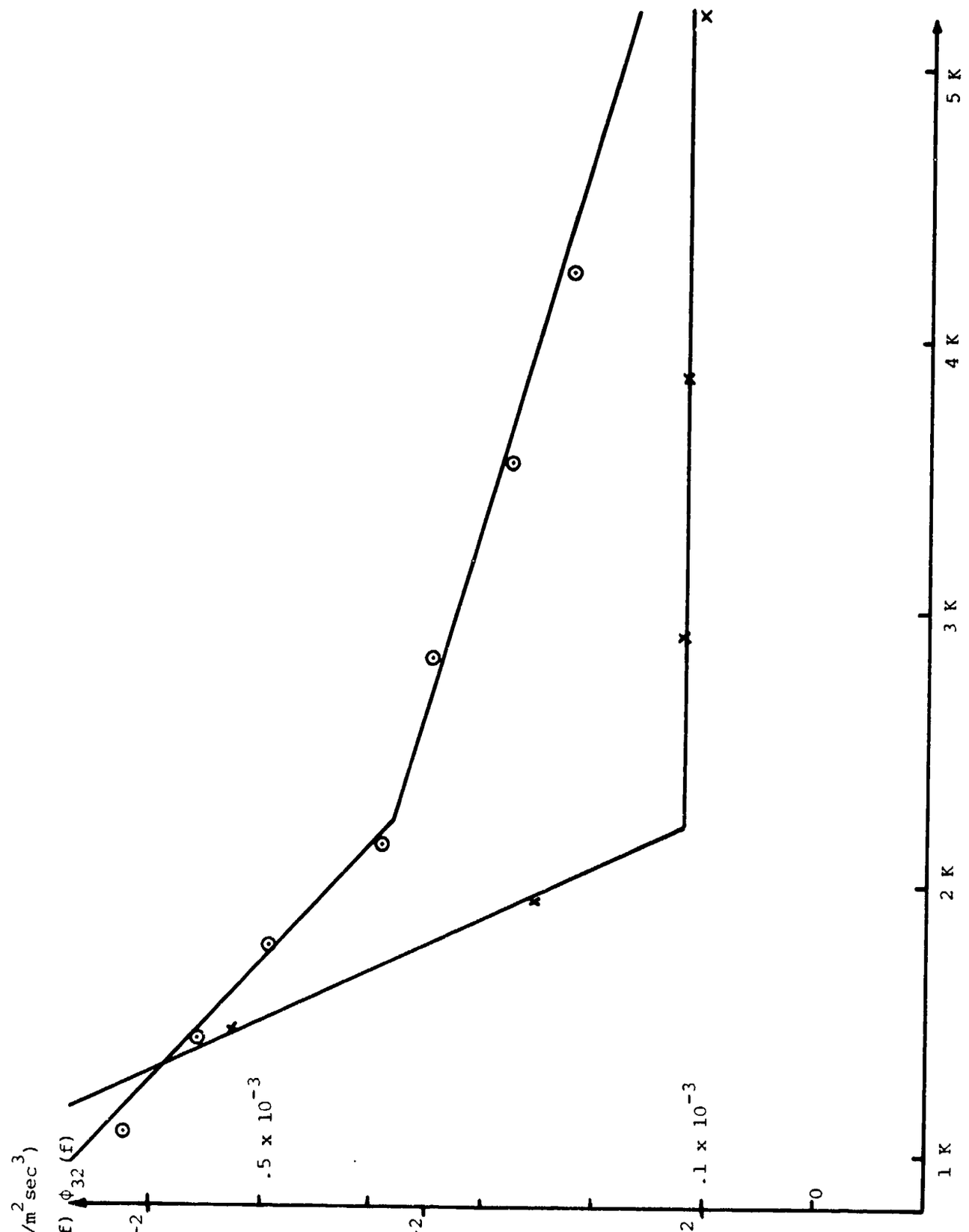

Figure 7.2 Wall pressure spectral density, $\phi_{U_\infty}(f)$, and its linear approximations. "o", U_∞ = 32 m/sec; "x", U_∞ = 48 m/sec.

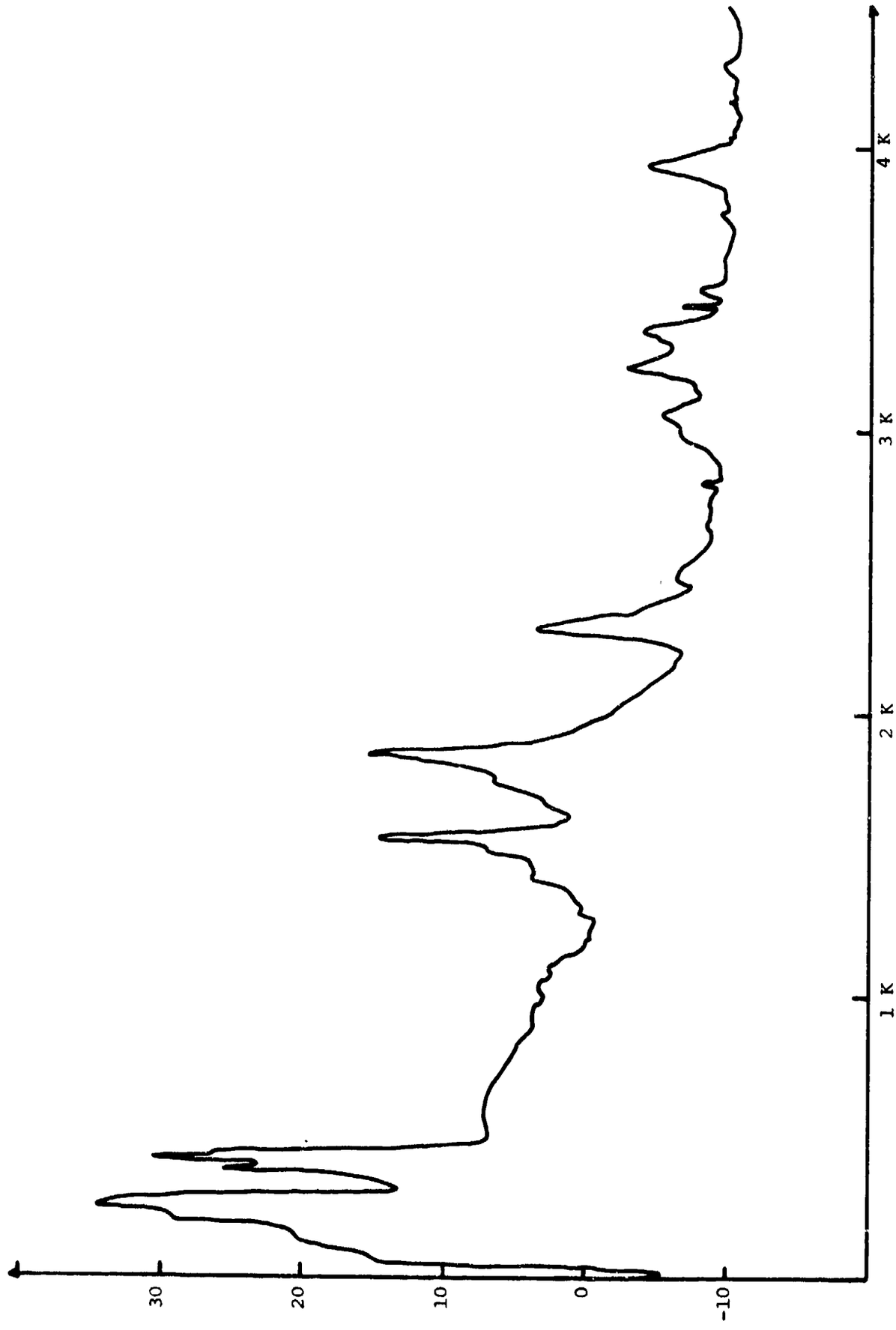

Figure 8.1a Displacement level in 10 Hz band width.

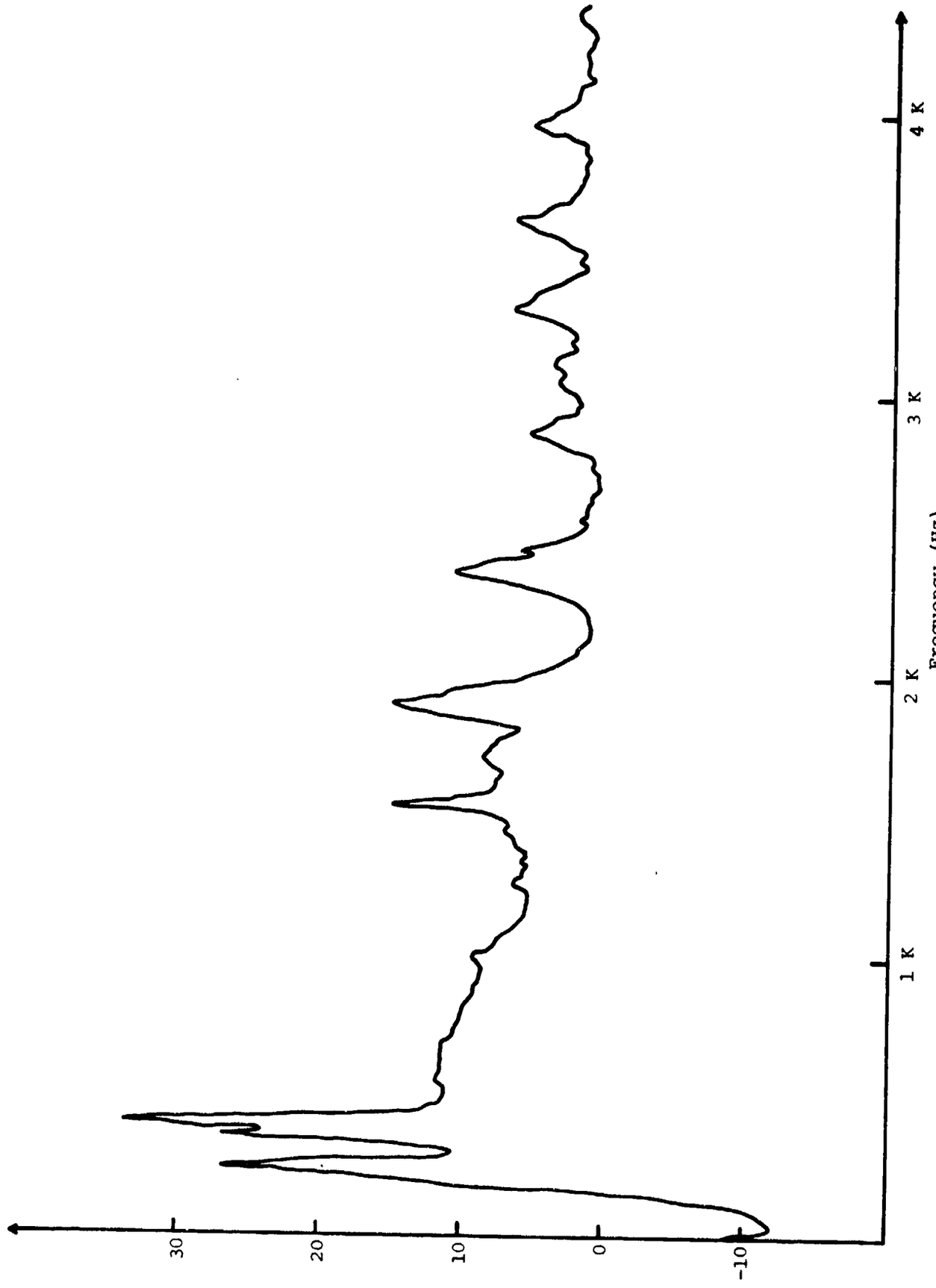

Figure 8.1b Displacement level in 10 Hz band width

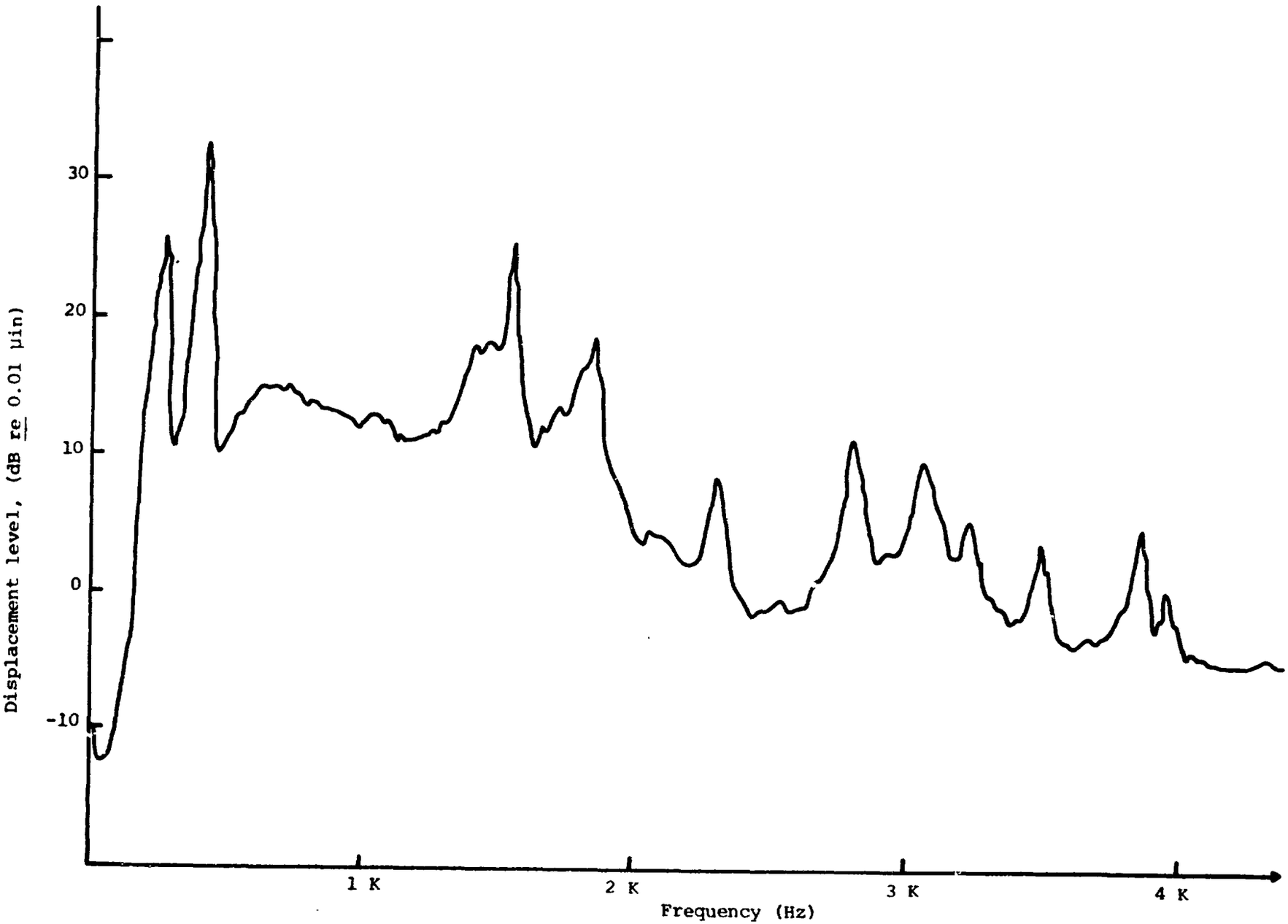

Figure 8.1c Displacement level in 10 Hz band width

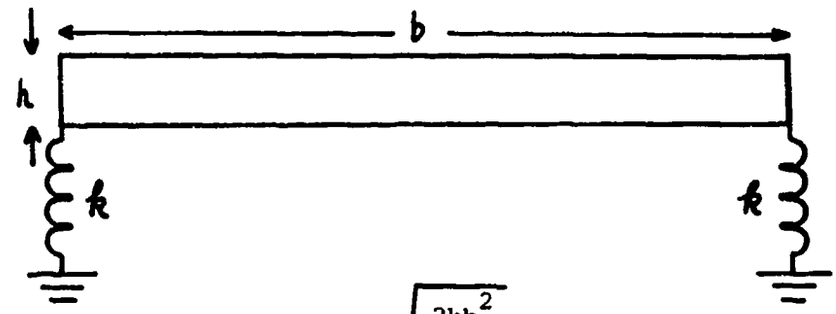

Pitching modal frequency, $\Omega = \sqrt{\frac{2kb^2}{4I}}$

Heaving modal frequency, $\omega = \sqrt{\frac{2k}{M}}$

$\frac{\Omega}{\omega} = \sqrt{\frac{Mb^2}{4I}} = \sqrt{3} = 1.73$

FIGURE 8.2 Ratio Between Pitching and Heaving Resonant Frequencies for a Bar Resting on Two Strings.

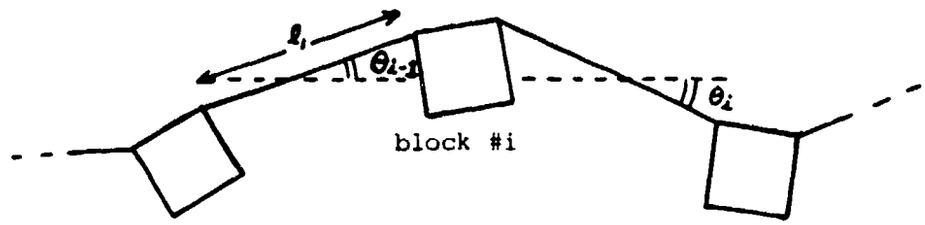

FIGURE 8.3 String and Block Model Excited Below Foundamental Resonant Frequency of a $\ell_1 \times \ell_3$ Membrane Unit.